NATIONAL ADVISORY COMMITTEE FOR AERONAUTICS

WARTIME REPORT

ORIGINALLY ISSUED

June 1944 as
Memorandum Report

AERODYNAMIC TESTS OF AN AN-M-65-AZON 1000-POUND RADIO-CONTROLLED BOMB IN THE LMAL 16-FOOT HIGH-SPEED TUNNEL

By E. O. Pearson, Jr.

Langley Memorial Aeronautical Laboratory
Langley Field, Va.

NACA

WASHINGTON

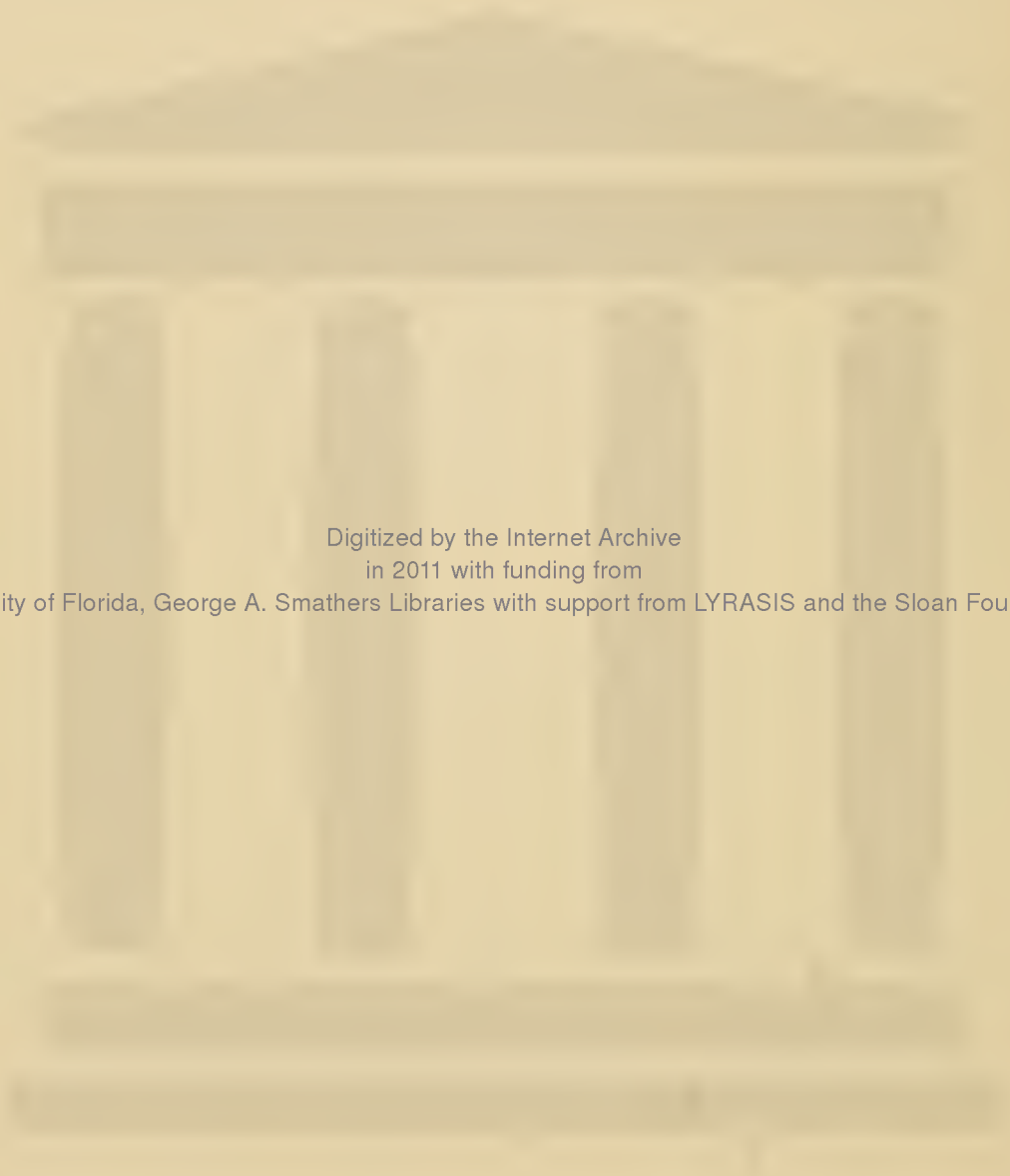

NATIONAL ADVISORY COMMITTEE FOR AERONAUTICS

MEMORANDUM REPORT

for the

Army Air Forces, Materiel Command

AERODYNAMIC TESTS OF AN AN-M-65-AZON 1000-POUND RADIO-CONTROLLED BOMB IN THE LMAL 16-FOOT HIGH-SPEED TUNNEL

By E. O. Pearson, Jr.

SUMMARY

Tests were made in the LMAL 16-foot high-speed tunnel to determine the aerodynamic characteristics of a 1000-pound AN-M-65-AZON radio-controlled bomb at Mach numbers ranging from 0.2 to 0.6.

Over the Mach number range covered in the tests the hinge-moment coefficients, yawing-moment coefficients, and lateral-force coefficients exhibited no important changes with increasing speed. The drag coefficients increased gradually with increasing Mach number but no sudden increases were observed. The effect on the bomb aerodynamic characteristics of antenna struts mounted on the bomb tail was found to be small.

The rudder and aileron operating mechanisms were found to be capable of supplying several times the required torques for maximum control deflections at a Mach number of 0.6 at sea level. The operating mechanism is also adequate for maximum control deflections at a Mach number of 1.0 provided that no appreciable increases in hinge-moment coefficient occur between M = 0.6 and M = 1.0. However, because of uncertainty as to the value of the hinge-moment coefficient at or near M = 1.0, the desirability of providing more powerful control mechanisms was indicated.

INTRODUCTION

Tests have been conducted in the LMAL 16-foot high-speed tunnel to determine the aerodynamic

characteristics of a 1000-pound AN-M-65-AZON radio-controlled bomb. Measurements of rudder hinge moment, yawing moment, lateral force, and drag were made at a number of tunnel speeds up to a Mach number of about 0.6 which corresponds to a speed of 670 feet per second at sea level.

Aerodynamic tests of a two-thirds scale model of a similar bomb were conducted previously at the Daniel Guggenheim Airship Institute at Akron, Ohio. These tests, however, were made at low airspeeds and, therefore, uncertain extrapolations of the data to the high-speed operating conditions were necessary in the design of the control mechanism and in performance computations.

In drop tests of the bombs it was found that, while some of the experimental bombs performed satisfactorily, a large percentage of the production version failed to respond properly to the control. The present investigation was undertaken principally to determine if the lack of control of the production bombs was due to adverse compressibility effects. It was also desired to obtain high-speed test data upon which to base performance calculations and the design of the control mechanism.

The investigation was undertaken at the request of the Army Air Forces, Materiel Command.

SYMBOLS AND DEFINITIONS

V	free-stream velocity, feet per second
a	speed of sound in air, feet per second
M	Mach number (V/a)
ρ	mass density of air, slugs per cubic foot
q	dynamic pressure, pounds per square foot $\left(\frac{1}{2}\rho V^2\right)$
M_H	hinge moment acting on one rudder, inch-pounds Positive hinge moments tend to change the rudder angle in a positive direction. (See sketch in figure 1 illustrating the sign conventions.)

d distance from rudder hinge axis to trailing edge of rudder, 4.81 inches

S area of one rudder, 0.282 square foot

C_H hinge-moment coefficient (M_H/qSd)

N yawing-moment, pound-feet
Positive yawing moments tend to change the angle of sideslip in a positive direction. (See fig. 1.)

F area of maximum cross section of bomb, 1.918 square feet

l over-all length of bomb, 5.613 feet

C_n yawing-moment coefficient (N/qFl)

Y lateral force, pounds

C_Y lateral-force coefficient (Y/qF)

D drag, pounds

C_{D_F} drag coefficient (D/qF)

ψ angle of sideslip, degrees
For positive angles the bomb nose is to the right of the line of flight.

δ_R rudder angle with respect to the neutral position, degrees
For positive angles the trailing edge is to the left.

The dimensions given above, together with other dimensions which might prove useful, are shown in figure 2.

DESCRIPTION OF BOMB AND APPARATUS

The AN-M-65-AZON bomb consists of a standard M-65 bomb case to which is fitted a special tail unit equipped with movable control surfaces and housing a control mechanism capable of being operated remotely

by radio. The bomb can be controlled only in the left and right or azimuth direction, hence, the designation AZON an abbreviation of "azimuth only." A gyroscopic control mechanism operates the horizontal control surfaces differentially as ailerons to prevent the bomb from rolling in flight.

For these tests part of the control apparatus was removed from the tail and strain-gage equipment for measuring rudder hinge moments was installed. Since the ailerons and rudders were identical, hinge-moment data apply equally to both. For this reason no provision was made for measuring aileron hinge moments directly and the ailerons were locked in the neutral position throughout the tests.

In order to facilitate installation and testing the bomb was mounted in the tunnel in a position 90° in roll from its normal flight position so that rudders became elevators, yawing moments became pitching moments, etc. The results throughout the report, however, are given in terms consistent with the flight orientation.

The bomb was supported on the tunnel center line by means of a single vertical strut 8 inches in chord and of NACA section 16-009. The strut was shielded by a fairing of the same section to within about 10 inches of the bomb case. In addition, four 0.080-inch wires were attached to the bomb to provide lateral support. The wires and support strut were mounted on the balance frame and were included in the force measurements. A photograph of the bomb installed in the tunnel is shown in figure 3.

The angle of sideslip of the bomb was variable from -20° to 20° through fixed increments by means of an internal indexing mechanism while the rudder angle was continuously variable from -20° to 20° by means of a slotted plate arrangement.

As received, the bomb tail was fitted with four struts which, in addition to serving as braces for the tail surfaces, also served as the radio antenna. The struts may be seen in figure 3.

TEST PROCEDURE

The test procedure consisted of measuring rudder hinge moment, yawing moment, lateral force, and drag at a number of speeds up to a Mach number of approximately 0.6 for each combination of rudder angle and angle of sideslip. In determining the bomb characteristics only the negative range of sideslip angles (0° to -20°) was investigated in order to keep the bomb tail outside the wake of the support strut and its fairing. The angular range of 0° to 20° was employed in determining the support-strut tares. The range of rudder angles tested was from -15° to 20°. Most of the test runs were made with the antenna tail struts installed but a few runs were made with the struts removed for purposes of comparison. This information on the effect of the antenna struts was specifically requested by the Army. The results throughout the report are given for the struts-installed configuration unless otherwise specifically noted.

During the tests deflections of the bomb in the direction of the air flow were measured and corrections to the yawing moment applied to account for the change in position. In addition, a calibration was later made to determine the angular deflections of bomb and rudders under the influence of the aerodynamic loads.

Strut tare forces were measured with the aid of an image strut mounted as shown in figure 4. Wire tare forces were determined simply by making measurements with the wires removed.

Yawing moment, lateral force, and drag data have been corrected both for tares and for the angular deflections of bomb and rudders under aerodynamic loads.

Corrections for the deflections have not been applied to the hinge-moment data. As presented the hinge-moment coefficient is about 9 percent too low at the greatest negative bomb and rudder angle and at the highest tunnel speed, which is the extreme case.

RESULTS AND DISCUSSION

Curves of yawing-moment coefficient, lateral-force coefficient, and drag coefficient versus Mach number are presented in figures 5 through 18. It should be pointed

out that the $\psi = -0.5^\circ$ and $\delta_R = 0^\circ$ curves shown in figures 5, 11, and 17 are believed to be slightly in error due to friction in the balance system during that particular test run. This is indicated by the scatter of the test points particularly at the lower speeds.

Derived curves of yawing moment, lateral force, and drag coefficients versus sideslip angle are given in figures 19, 20, and 21. Figure 22 shows the lateral force and drag coefficients at trim as a function of the rudder angle. The effect of center-of-gravity location on the stability and trim angles of the bomb is shown in figure 23. Hinge-moment data are presented in figures 24 through 31. Figure 32 is a photograph of a rudder after structural failure has occurred.

Yawing moment.- Yawing-moment coefficient data are presented in figures 5 through 10. During the tests yawing moments were measured about a point 22.58 inches from the bomb nose. In the data presented in the report the moments were transferred to a point 28.60 inches from the nose of the bomb, which was the center-of-gravity location of sand-filled bombs used in the drop tests, mentioned earlier in the report.

The figures show that the variation of the yawing-moment coefficient with Mach number is small for all the rudder angles and angles of sideslip over the range of speeds covered in this investigation. Figures 9 and 10 show the variation of yawing-moment coefficient with Mach number with the antenna struts removed. From a comparison of these figures with figures 5 and 7 it will be seen that the struts have practically no effect on the yawing-moment coefficient.

Lateral force.- Curves of lateral-force coefficient versus Mach number for the various rudder angles and angles of sideslip are presented in figures 11 through 16. In general, the coefficient increases negatively with increasing Mach number. The change is slight, however. Figures 15 and 16 show the variation of lateral-force coefficient with Mach number with the antenna struts removed. As in the case of the yawing-moment coefficients the effect of the struts on the lateral-force coefficient is small.

Drag.- The variation of drag coefficient with Mach number is shown in figure 17 for various angles of sideslip and rudder angles. No sudden increases in the drag

coefficient occurred in the speed range of the tests. Curves for a few of the sideslip and rudder angles have not been plotted in figure 17 to avoid excessive congestion and overlapping. Curves of the drag coefficient versus Mach number with the antenna tail struts removed are given in figure 18. A comparison of this figure with figure 17 shows that for a sideslip angle of -0.5° and a rudder angle of 0° removal of the struts results in a decrease in the drag coefficient of 0.009 or about 5 percent of the minimum drag.

Bomb characteristics as a function of sideslip angle.- Curves of yawing-moment coefficient, lateral-force coefficient, and drag coefficient versus the angle of sideslip are presented in figures 19, 20, and 21, respectively. These curves are cross plots of the faired yawing-moment, lateral-force, and drag coefficient curves previously presented. Since the variation of the coefficients with Mach number was not appreciable except for the drag coefficient only the curves for a Mach number of 0.6 are shown. It will be noted from figure 19 that the bomb stability decreases slightly as the angle of sideslip approaches zero. At the larger negative sideslip angles and positive rudder angles there is also some decrease in stability with increasing angle of sideslip.

Trim conditions.- Figure 22 shows the lateral-force and drag coefficients obtaining at trim for various rudder deflections. It will be seen that for the maximum rudder deflection of 20° and at a Mach number of 0.6 the bomb trims in an attitude for which the lateral-force coefficient is -0.422 and the drag coefficient is 0.360. Reference to figure 19 shows that the corresponding angle of sideslip for trim is -10.5°.

Bomb maneuverability.- The following table is presented to illustrate roughly the magnitude of the lateral deviations possible when the bomb is dropped from different altitudes. It is assumed that the bombing airplane is flying at a constant indicated airspeed of 175 miles per hour and that the maximum bomb rudder deflection of 20° is maintained over the entire flight path. The left-hand column gives the height above sea level which is also considered to be ground level and the right-hand column gives the approximate value of the maximum lateral deviation possible when the bomb is released at the corresponding altitude.

Altitude of release (ft)	Approximate maximum lateral deviation (ft)
5,000	600
10,000	1600
15,000	2800
20,000	4200
25,000	5800

Effect of changes in the center-of-gravity location.- Figure 23 shows the effect upon trim angle and stability of a change in the center-of-gravity location 2 inches backward or forward from the 28.6-inch point. A more rearward location of the center of gravity results in a reduction in stability and an increase in the angle of sideslip for trim with a consequent increase in the lateral-force coefficient. A location forward of the 28.6-inch point results, of course, in the opposite effect.

With the data presented yawing-moment coefficients may be transferred from the 28.6-inch point to any new point by the relation

$$C_n = C_{n_{28.6}} + \left(C_Y \cos \psi\right)\frac{x}{d} + \left(C_{D_F} \sin \psi\right)\frac{x}{d}$$

where x is the distance from the 28.6-inch point to the new point measured along the bomb longitudinal axis. The value of x is positive if the new point is to the rear of the 28.6-inch point and negative if to the front.

Hinge moment.- Rudder hinge-moment data are presented in figures 24 through 31. Figures 24 through 27 show the variation of rudder hinge-moment coefficient with Mach number for various rudder angles and angles of sideslip. It may be seen that for the smaller angles of sideslip and rudder angles there is little variation of the hinge-moment coefficient with Mach number. The change becomes more pronounced for the larger angles but is not important in any case over the range of speeds covered in the tests. It is clear that any loss of control of the bomb at Mach numbers of 0.6 and below cannot be attributed to radical changes in hinge moments due to compressibility effects. Figure 28 shows the variation of hinge-moment coefficient with rudder angle for various angles of sideslip and

Mach numbers. Figures 29 and 30 show the variation of hinge-moment coefficient with Mach number with the antenna struts removed. Figure 31 shows the variation of hinge-moment coefficient with rudder angle for the same configuration. A comparison of these figures with figures 24, 26, and 28 shows that the struts have no appreciable effect on the rudder hinge-moment coefficient.

From tests in the LMAL Instrument Research Division on the rudder and aileron operating mechanisms it has been determined that the maximum torque available for holding the rudders in a given position is 200 inch-pounds. For a rudder deflection of 20° and the corresponding angle of sideslip for trim of -10.5° the total hinge moment acting on both rudders at a Mach number of 0.6 at sea level is 52 inch-pounds. If it is assumed that no change in the hinge-moment coefficient occurs between $M = 0.6$ and $M = 1.0$, the torque required at a Mach number of 1.0 is 145 inch-pounds. Such an assumption is somewhat doubtful, however, and if appreciable increases in the hinge-moment coefficient do occur, then at or near a Mach number of 1.0 at sea level the torque may be insufficient to maintain the maximum rudder deflection of 20°.

For the maximum aileron deflection of ±6° and an angle of sideslip of -0.5° the torque required for one aileron at a Mach number of 0.6 at sea level is 11 inch-pounds. Assuming as before that no change in the hinge-moment coefficient occurs between $M = 0.6$ and $M = 1.0$ the torque required at $M = 1.0$ is 30 inch-pounds. The maximum aileron torque available at the 6° deflection was determined to be 40 inch-pounds. Although the assumption of no change in the hinge-moment coefficient between $M = 0.6$ and $M = 1.0$ is more reasonable for the case of the small aileron deflection than for the larger rudder deflection, the margin of torque available over torque required at the higher speeds is not large in any case.

It would thus appear desirable from the foregoing considerations to employ both aileron and rudder operating mechanisms more conservative with regard to torque available.

Rudder failure.- During a routine inspection of the bomb upon completion of a test run it was found that failure of one of the rudders had occurred along the

spot-welded skin joint at the hinge axis. Up to the time the failure was discovered 33 test runs, each of about 45 minutes duration, had been completed. The failure appeared to be due to fatigue. Figure 32 is a photograph of the broken rudder.

CONCLUSIONS

Aerodynamic tests of a 1000-pound AZON bomb at Mach numbers ranging from 0.2 to 0.6 have indicated the following conclusions:

1. There were no appreciable compressibility effects on the rudder hinge-moment coefficients, the yawing-moment coefficients, or on the lateral-force coefficients. The drag coefficients increased gradually but no sudden increases occurred.

2. Removal of the antenna struts from the tail had only a slight effect on the aerodynamic characteristics.

3. The torques supplied by the rudder and aileron operating mechanisms were found to be several times the torques required at a Mach number of 0.6 at sea level for maximum control deflections. If no appreciable increases in the hinge-moment coefficient occur between $M = 0.6$ and $M = 1.0$, the available torque will be adequate at a Mach number of 1.0. Because of some uncertainty regarding the hinge-moment coefficient at $M = 1.0$, however, it would appear desirable to employ rudder and aileron operating mechanisms having greater available torque.

Langley Memorial Aeronautical Laboratory
National Advisory Committee for Aeronautics
Langley Field, Va., June 16, 1944

Ernest O. Pearson, Jr.

Ernest O. Pearson, Jr.
Aeronautical Engineer

Approved:

John Stack
Chief of Compressibility Research Division

ES

FIGURE LEGENDS

Figure 1.- Sketch showing sign conventions for angles, forces and moments.

Figure 2.- Sketch showing dimensions of AN-M-65-AZON bomb.

Figure 3.- AN-M-65-AZON 1000-pound bomb installed in the 16-foot high-speed tunnel.

Figure 4.- Setup employed for determining support-strut tares.

Figure 5.- Variation of yawing-moment coefficient with Mach number for several rudder angles $\Psi = -.5^\circ$.

Figure 6.- Variation of yawing-moment coefficient with Mach number for several rudder angles $\Psi = -10.5^\circ$.

Figure 7.- Variation of yawing-moment coefficient with Mach number for several rudder angles $\Psi = -15.5^\circ$.

Figure 8.- Variation of yawing-moment coefficient with Mach number for several rudder angles $\Psi = -20.5^\circ$.

Figure 9.- Variation of yawing-moment coefficient with Mach number for several rudder angles $\Psi = .5^\circ$; antenna struts removed.

Figure 10.- Variation of yawing-moment coefficient with Mach number for several rudder angles $\Psi = -15.5^\circ$; antenna struts removed.

Figure 11.- Variation of lateral-force coefficient with Mach number for several rudder angles $\Psi = -.5^\circ$.

Figure 12.- Variation of lateral-force coefficient with Mach number for several rudder angles $\Psi = -10.5^\circ$.

Figure 13.- Variation of lateral-force coefficient with Mach number for several rudder angles $\Psi = -15.5^\circ$.

Figure 14.- Variation of lateral-force coefficient with Mach number for several rudder angles $\Psi = -20.5^\circ$.

Figure 15.- Variation of lateral-force coefficient with Mach number for several rudder angles $\Psi = -.5^\circ$; antenna struts removed.

Figure 16.- Variation of lateral-force coefficient with Mach number for several rudder angles $\Psi = -15.5^\circ$; antenna struts removed.

Figure 17.- Variation of drag coefficient with Mach number for several angles of sideslip and rudder angles.

Figure 18.- Variation of drag coefficient with Mach number; antenna struts removed.

Figure 19.- Variation of yawing-moment coefficient with angle of sideslip for several rudder angles $M = 0.6$.

Figure 20.- Variation of lateral-force coefficient with angle of sideslip for several rudder angles $M = 0.6$.

Figure 21.- Variation of drag coefficient with angle of sideslip for several rudder angles $M = 0.6$.

Figure 22.- Drag and lateral-force coefficients at trim versus the rudder angle for several Mach numbers.

Figure 23.- Variation of yawing-moment coefficient with angle of sideslip for three center-of-gravity locations $M = 0.6$.

Figure 24.- Variation of rudder hinge-moment coefficient with Mach number for several rudder angles $\psi = -0.5°$.

Figure 25.- Variation of rudder hinge-moment coefficient with Mach number for several rudder angles $\psi = -10.5°$.

Figure 26.- Variation of rudder hinge-moment coefficient with Mach number for several rudder angles $\psi = -15.5°$.

Figure 27.- Variation of rudder hinge-moment coefficient with Mach number for several rudder angles $\psi = -20.5°$.

Figure 28.- Variation of rudder hinge-moment coefficient with rudder angle for several angles of sideslip and Mach numbers.

Figure 29.- Variation of rudder hinge-moment coefficient with Mach number for several rudder angles $\psi = -0.5°$; antenna struts removed.

Figure 30.- Variation of rudder hinge-moment coefficient with Mach number for several rudder angles $\psi = -15.5°$; antenna struts removed.

Figure 31.- Variation of rudder hinge-moment coefficient with rudder angle; antenna struts removed.

Figure 32.- Rudder failure.

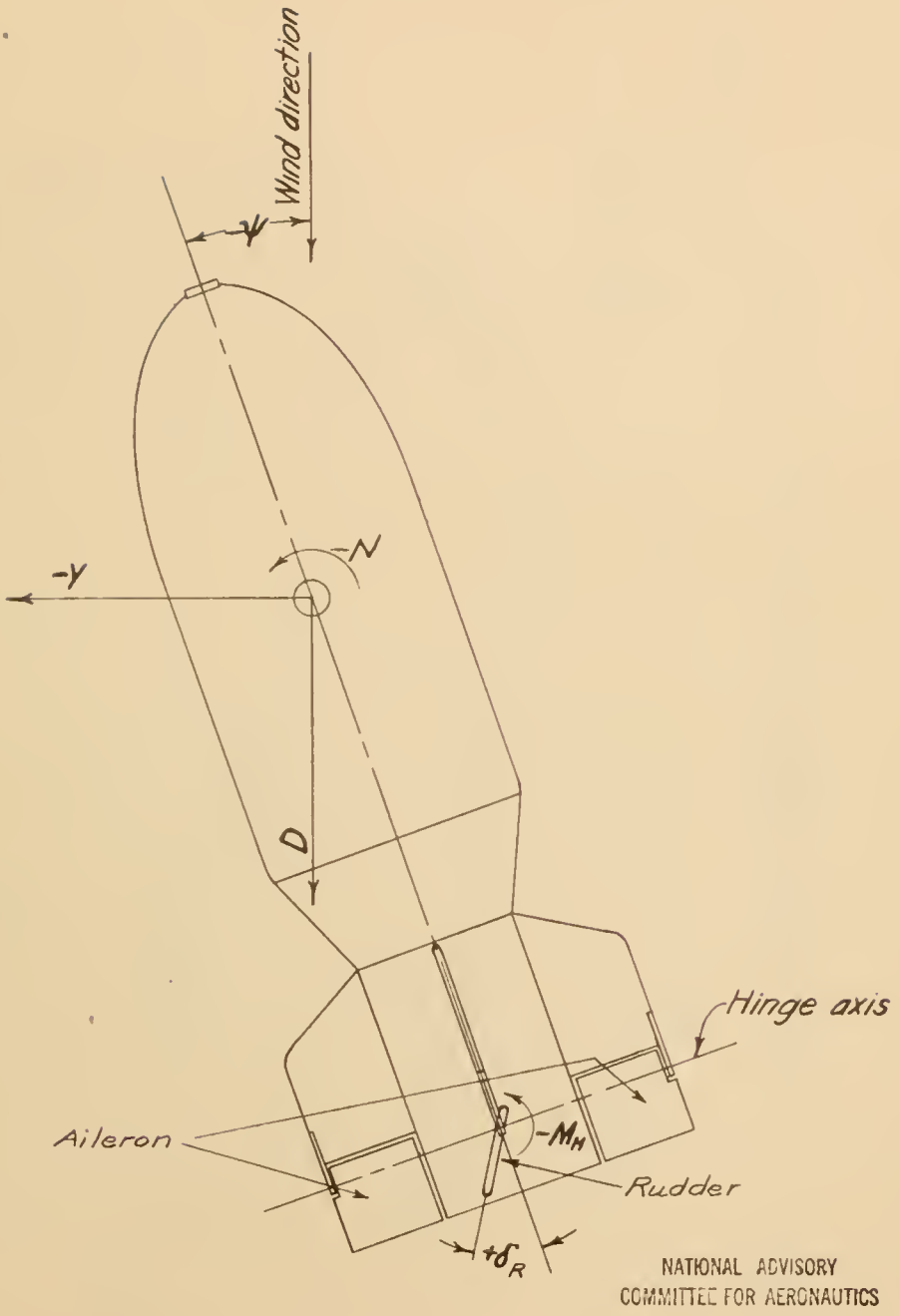

Figure 1.– Sketch showing sign conventions for angles, forces, and moments.

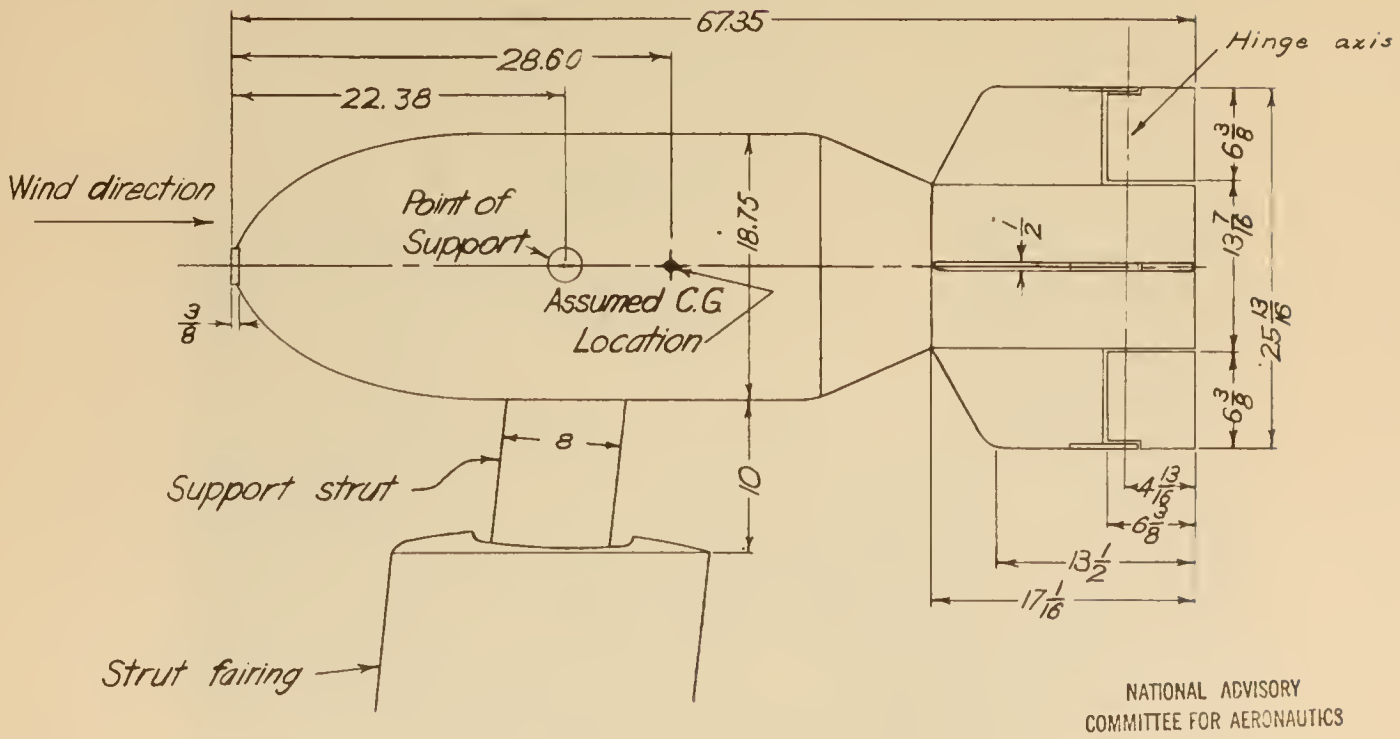

All dimensions are in inches

Figure 2.- Sketch showing dimensions of AN-M-65-AZON Bomb.

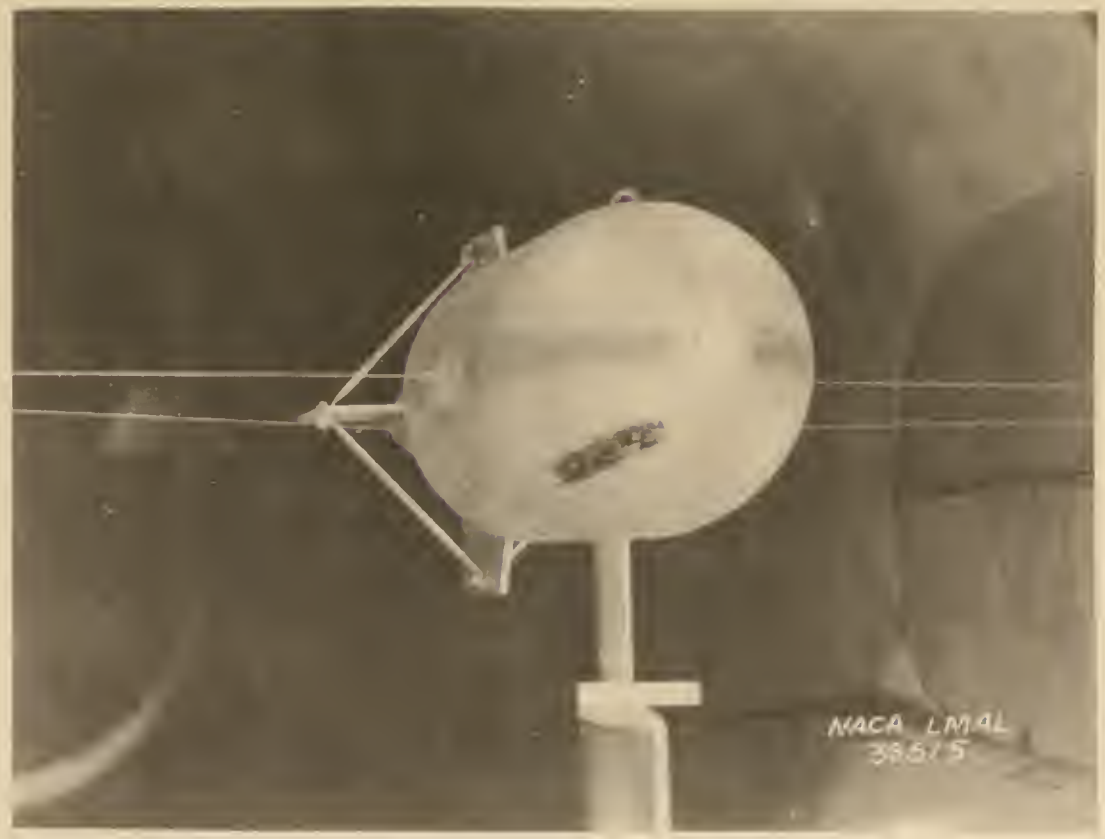

Figure 3.- AN-M-65-AZON 1000-pound bomb installed in the 16-foot high-speed tunnel.

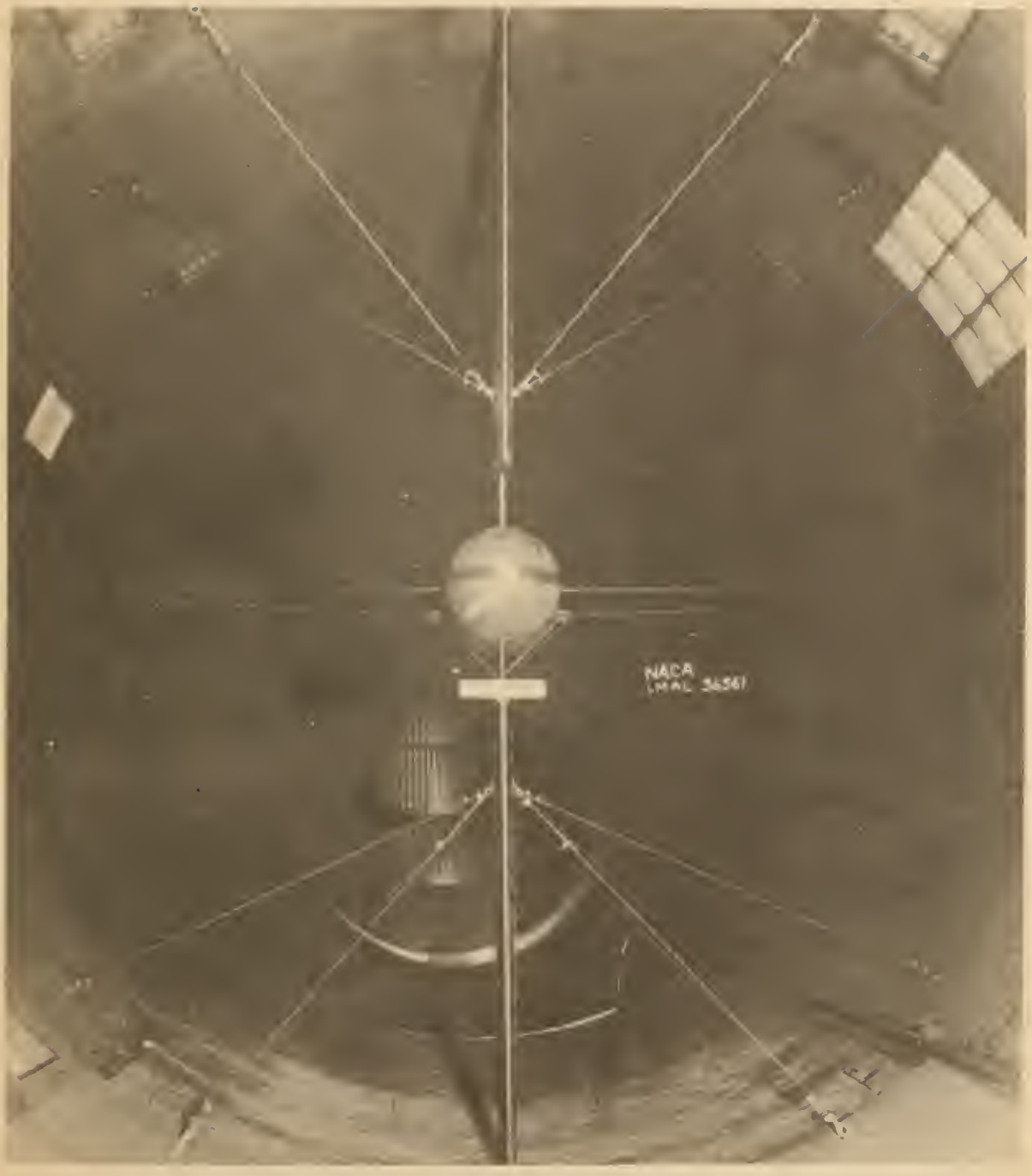

Figure 4.- Setup employed for determining support-strut tares.

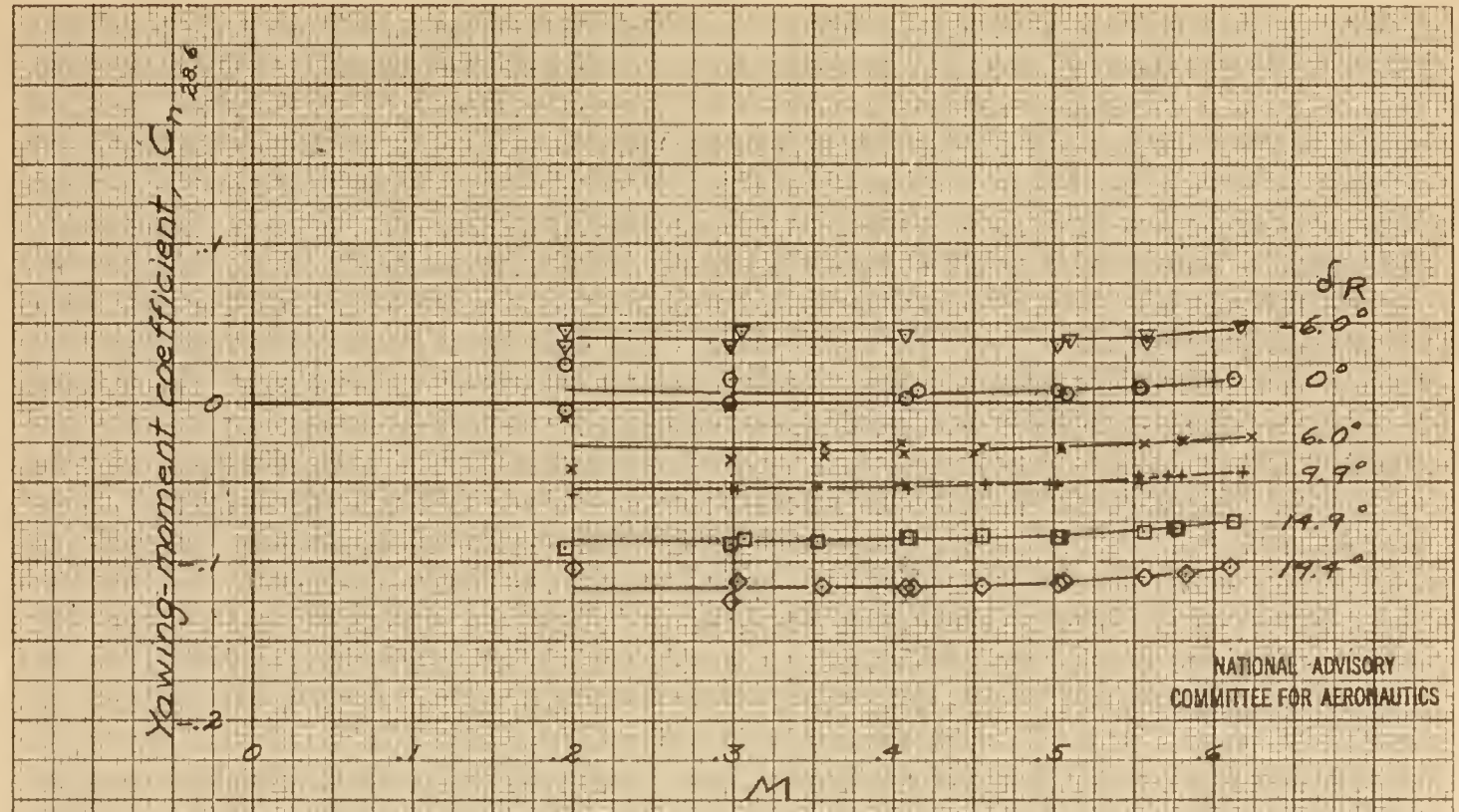

Figure 5.- Variation of yawing-moment coefficient with Mach number for several rudder angles $\psi = \pm .5°$

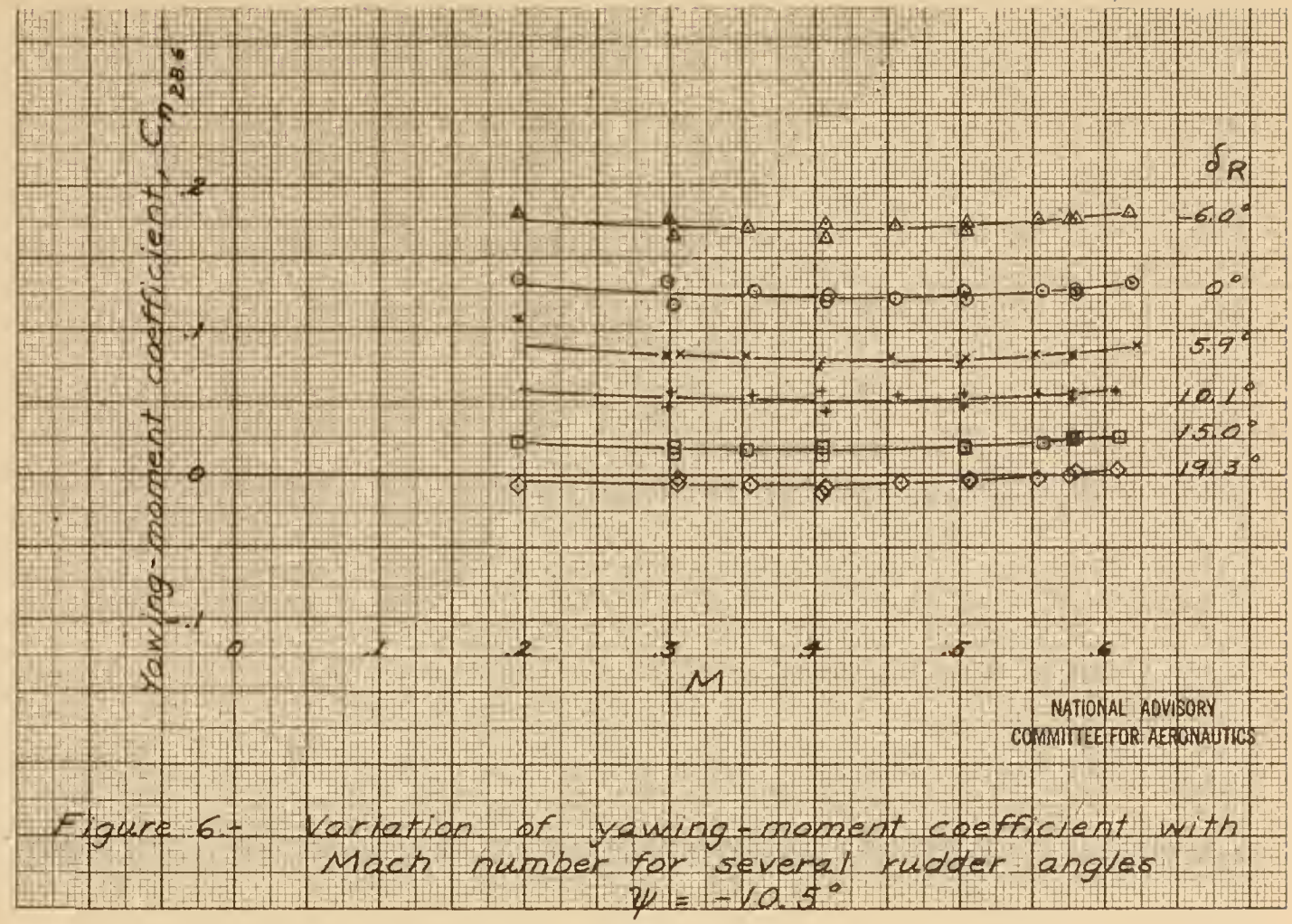

Figure 6.- Variation of yawing-moment coefficient with Mach number for several rudder angles $\psi = -10.5°$

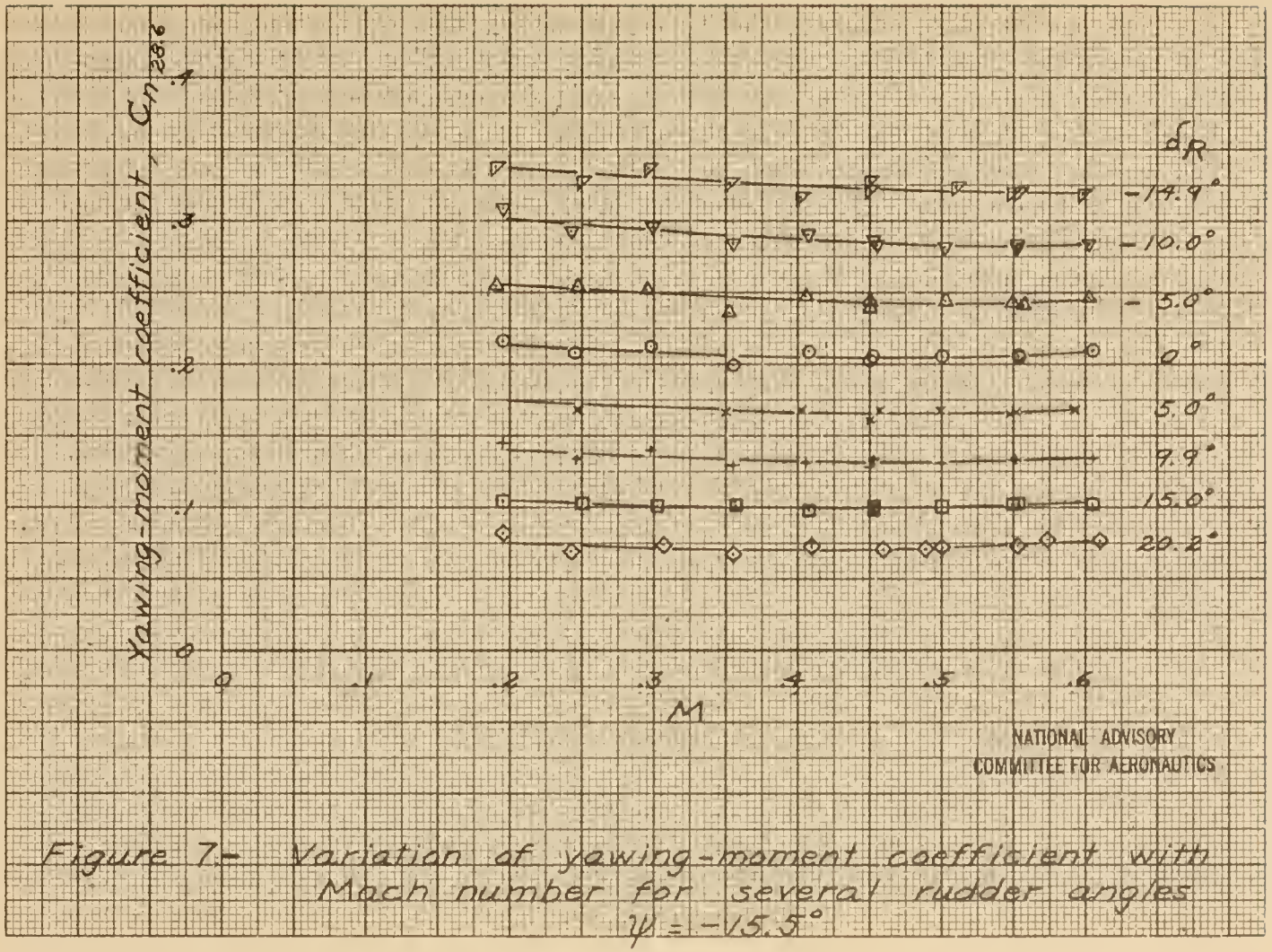

Figure 7.— Variation of yawing-moment coefficient with Mach number for several rudder angles $\psi = -15.5°$

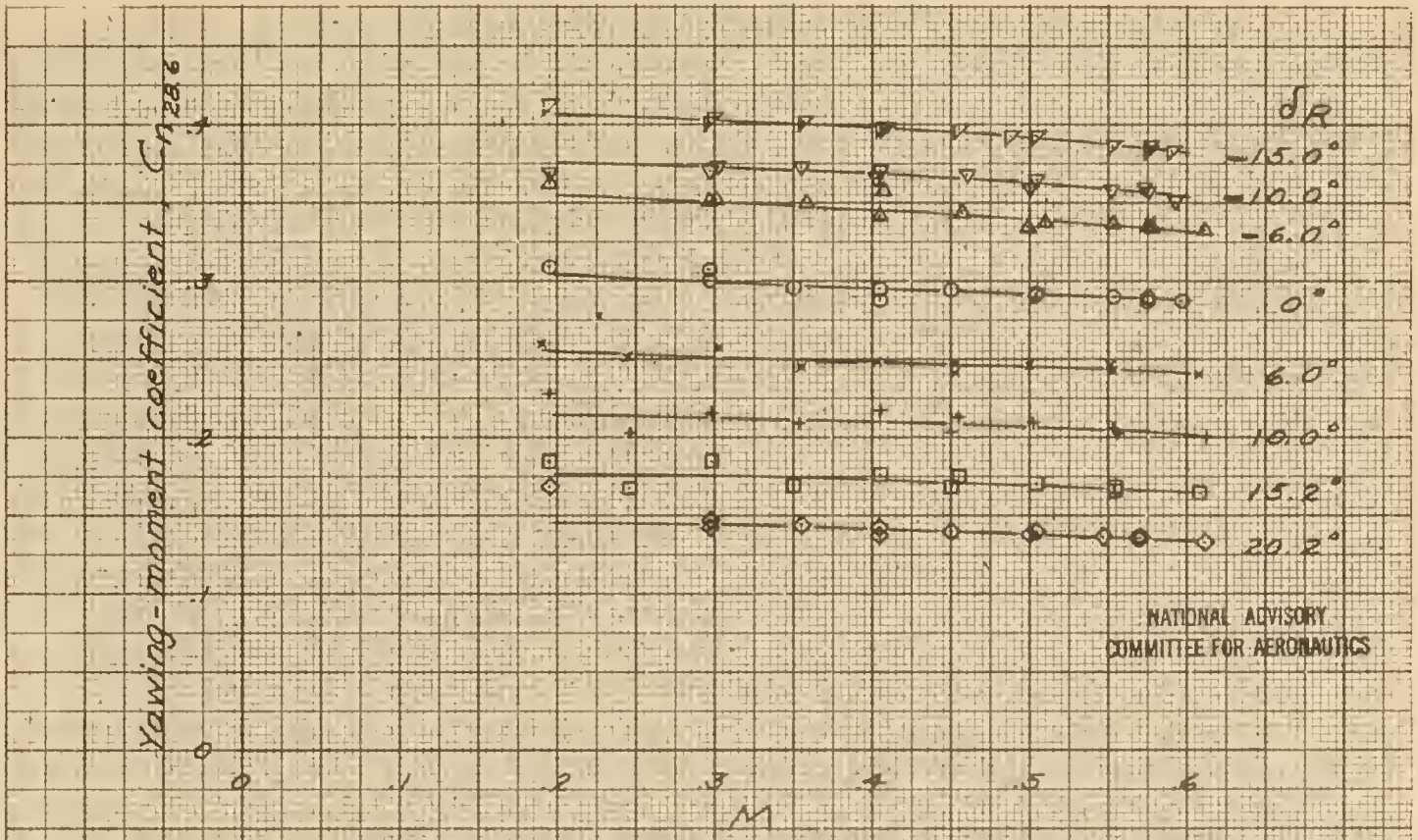

Figure 8.- Variation of yawing-moment coefficient with Mach number for several rudder angles $\psi = -20.5°$

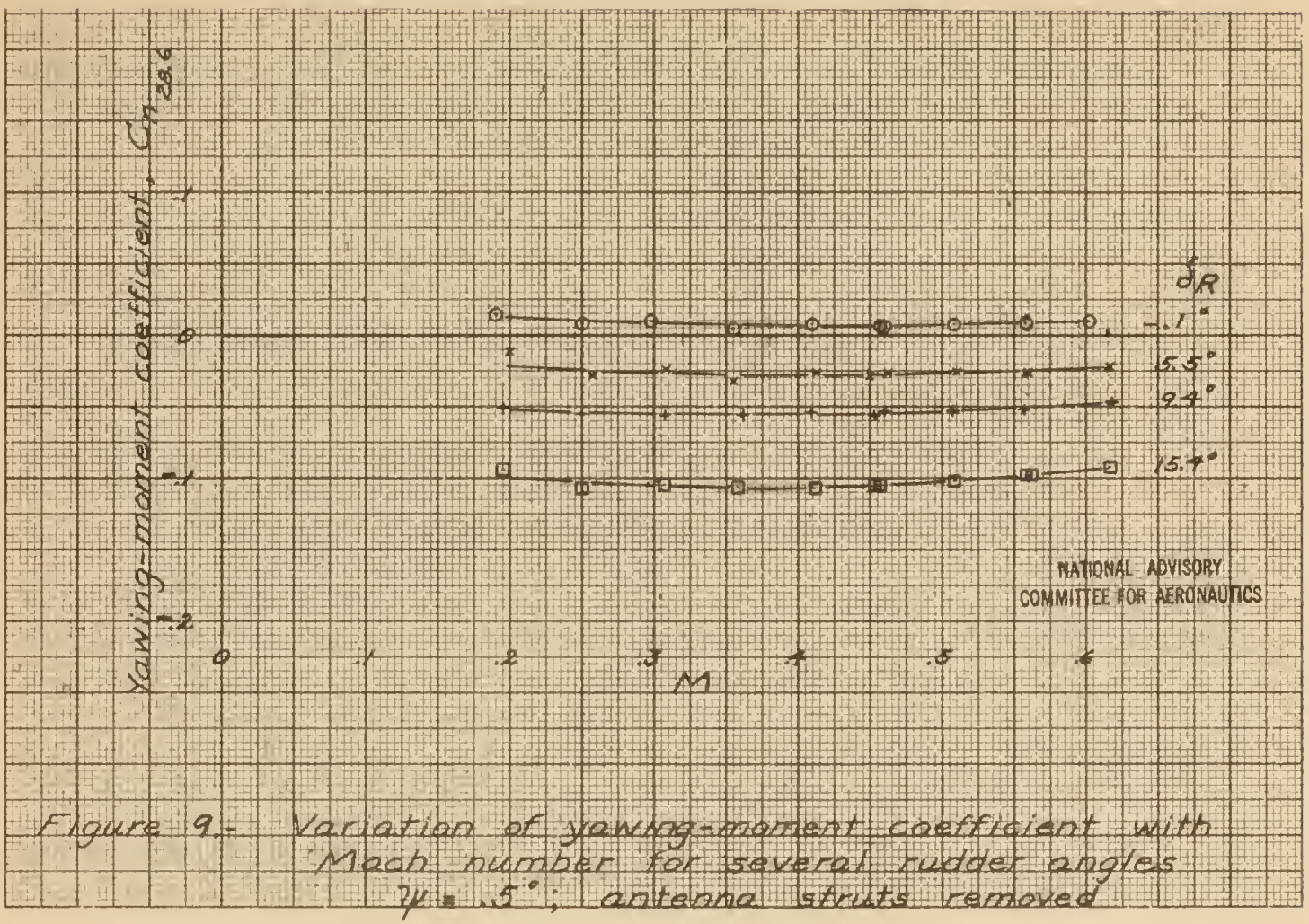

Figure 9.- Variation of yawing-moment coefficient with Mach number for several rudder angles $\psi = .5°$; antenna struts removed

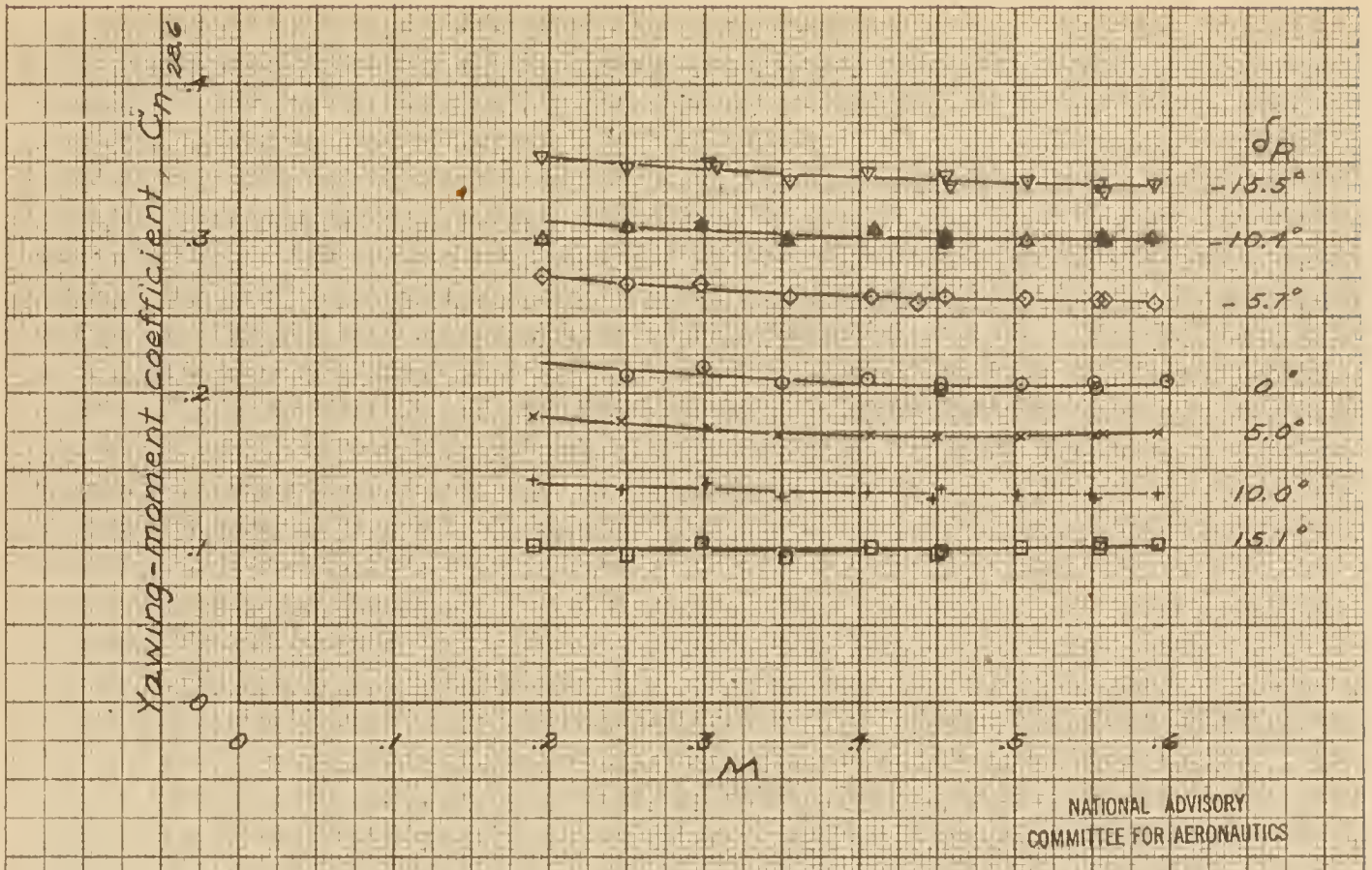

Figure 10- Variation of yawing-moment coefficient with Mach number for several rudder angles $\psi = -15.5°$; antenna struts removed

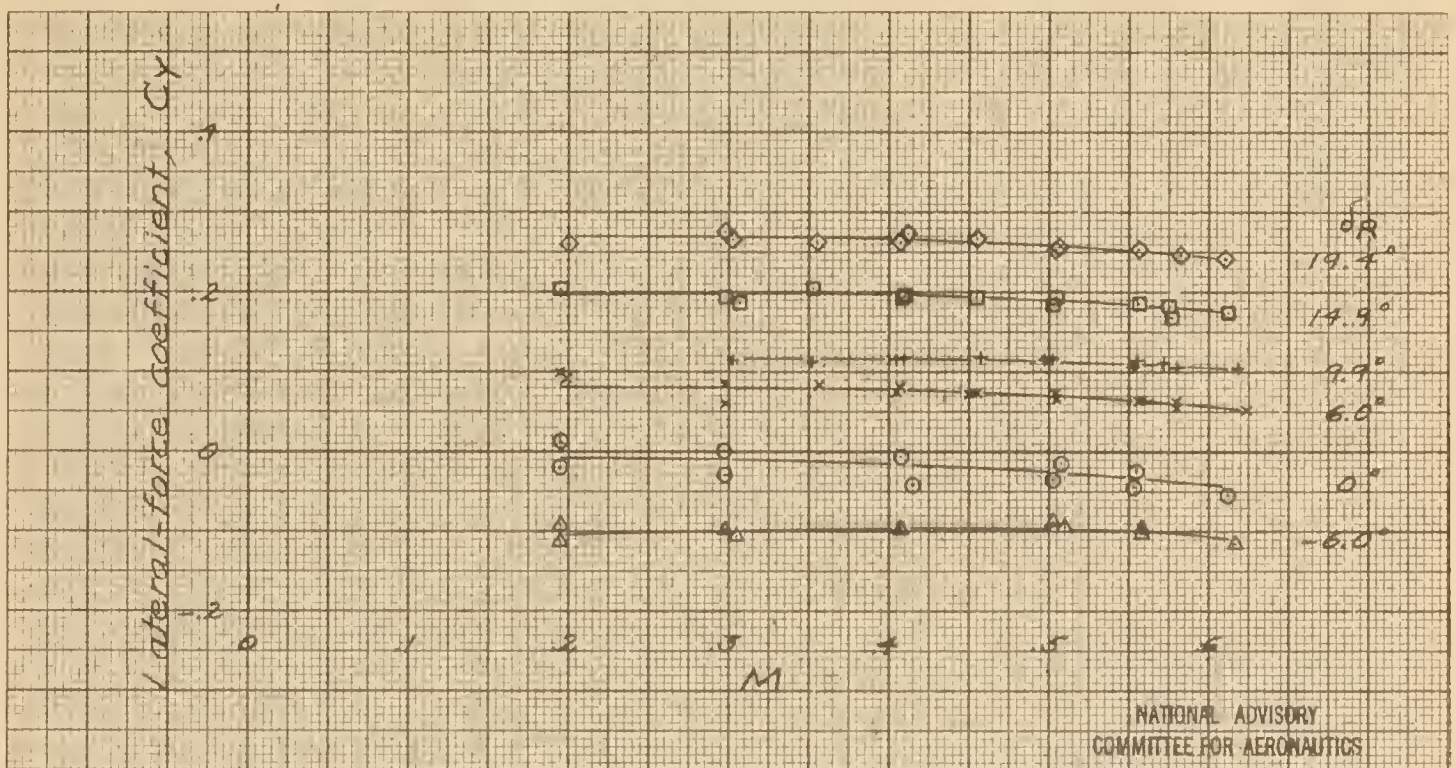

Figure 11.- Variation of lateral-force coefficient with Mach number for several rudder angles $\psi = -5°$

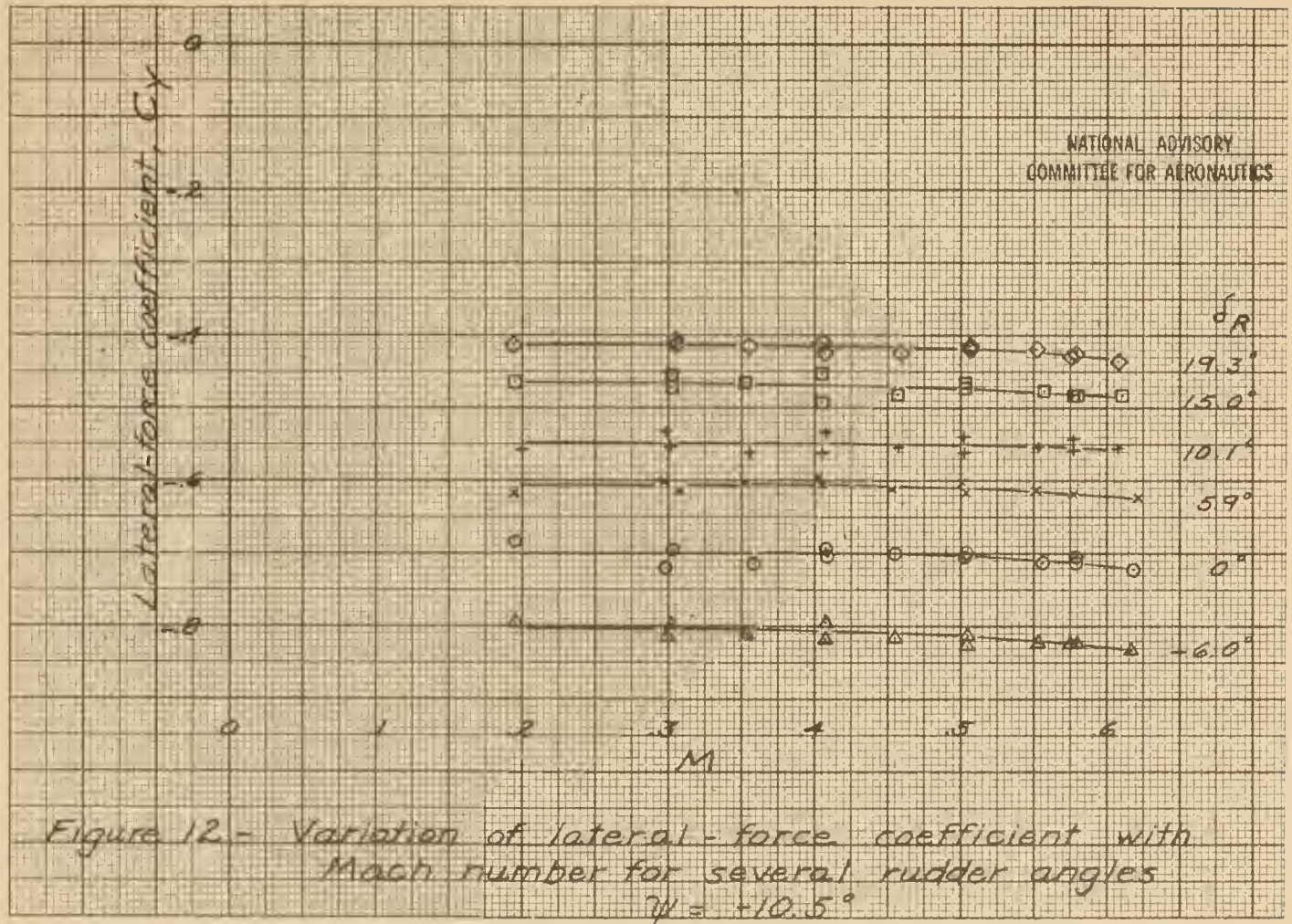

Figure 12.- Variation of lateral-force coefficient with Mach number for several rudder angles $\psi = -10.5°$

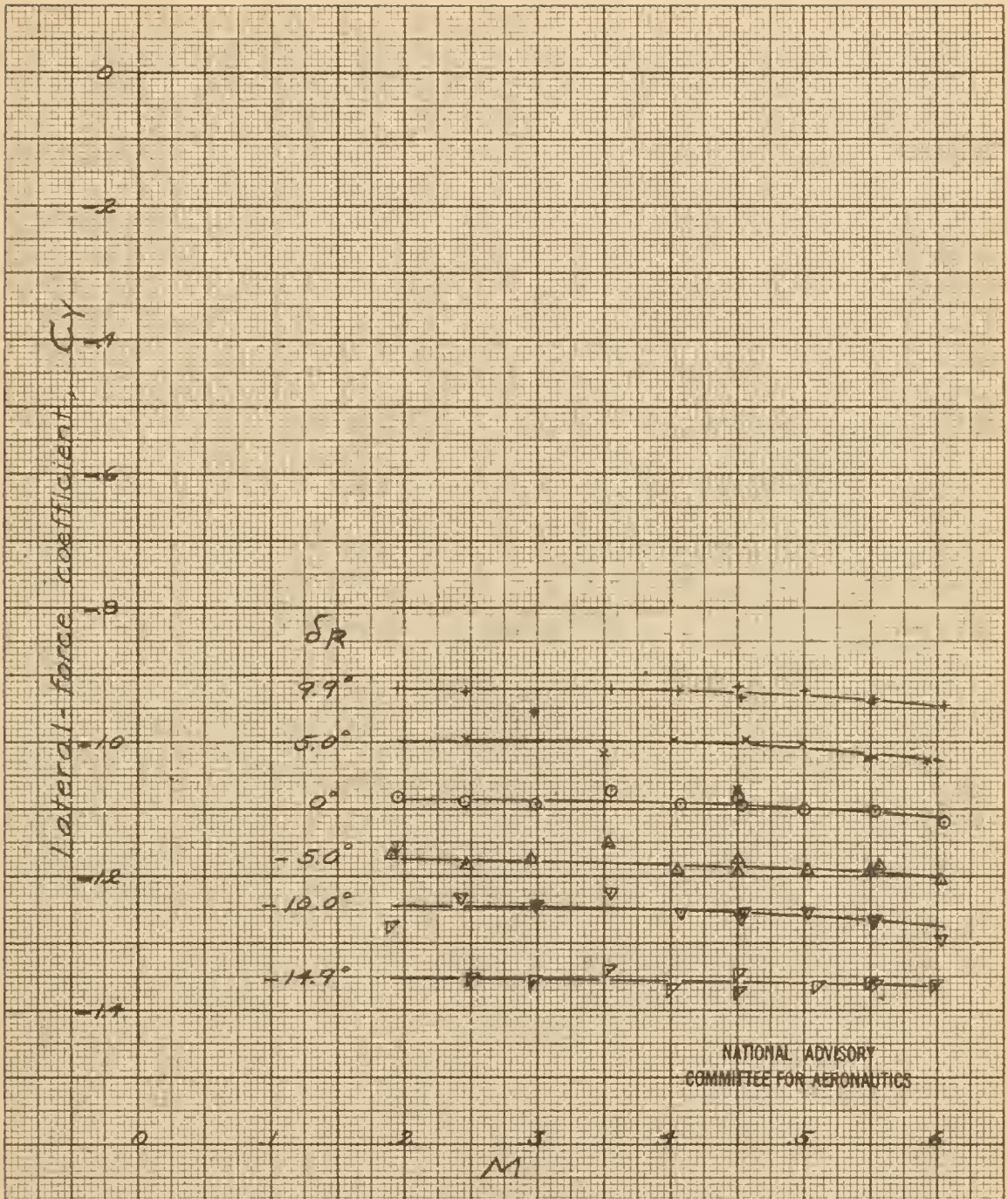

Figure 13.- Variation of lateral-force coefficient with Mach number for several rudder angles $\psi = -15.5°$

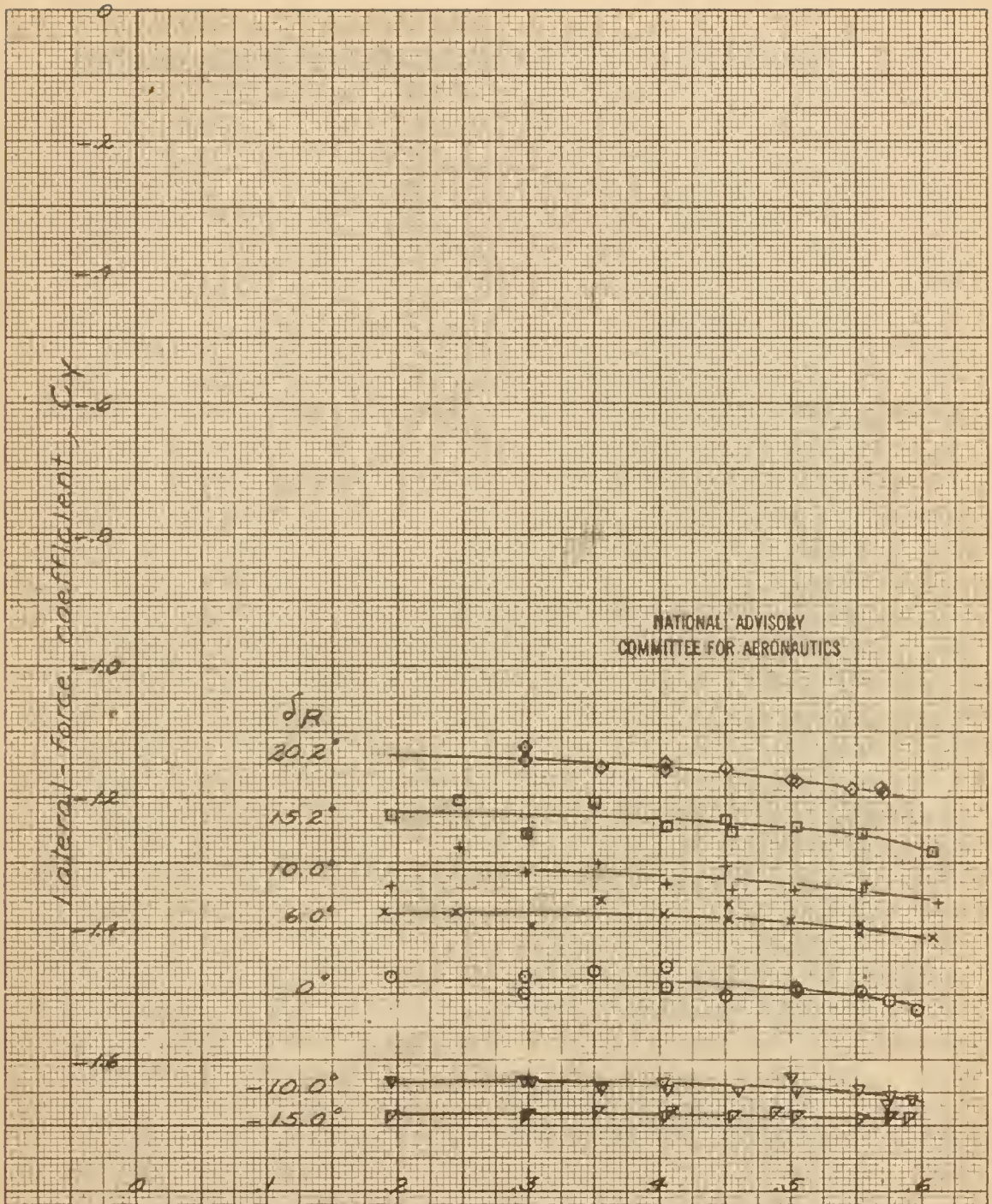

Figure 14.- Variation of lateral-force coefficient with Mach number for several rudder angles $\psi = -20.5°$

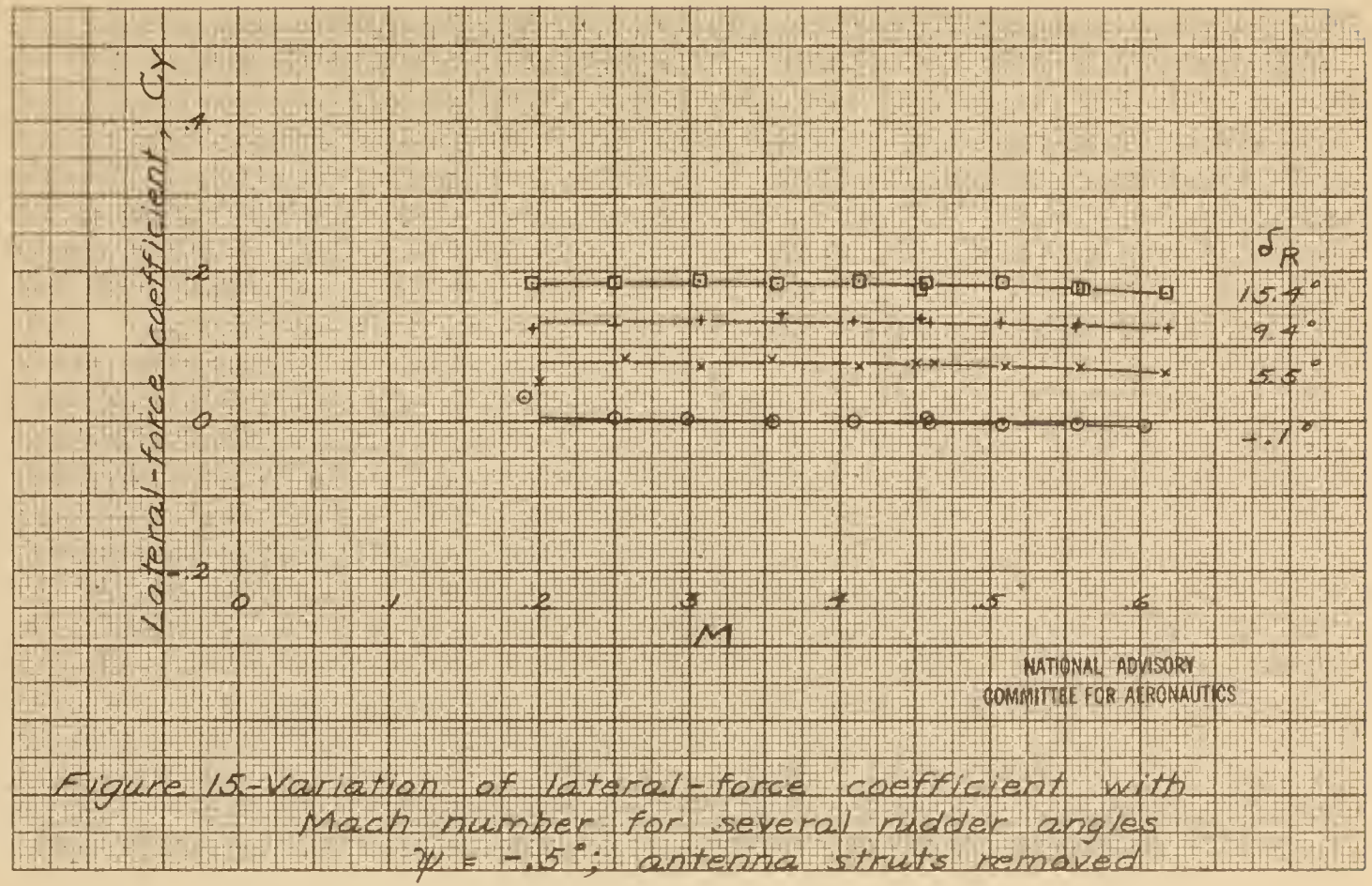

Figure 15.-Variation of lateral-force coefficient with Mach number for several rudder angles $\psi = -.5°$; antenna struts removed

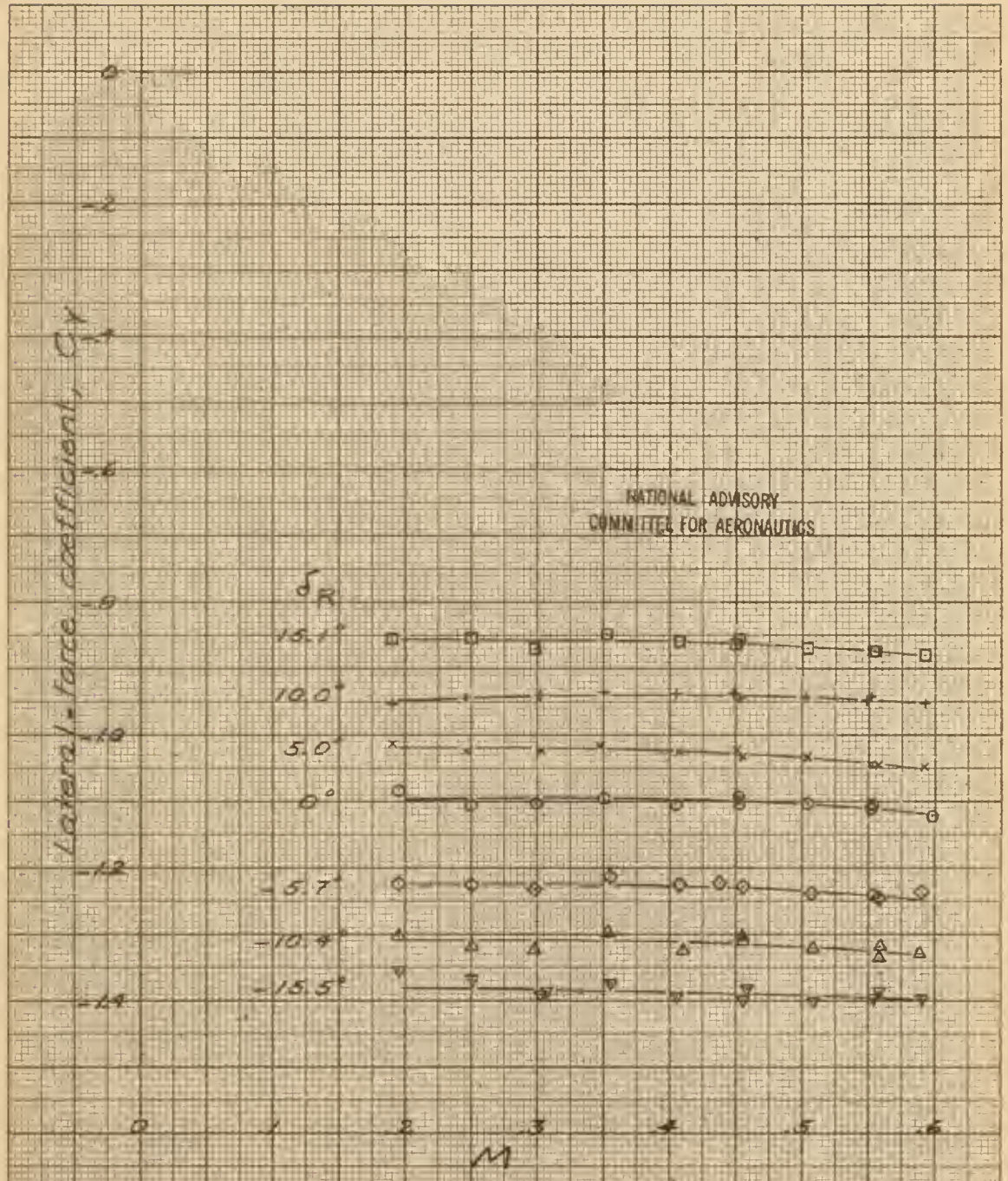

Figure 16.- Variation of lateral-force coefficient with Mach number for several rudder angles $\psi = -15.5°$; antenna struts removed

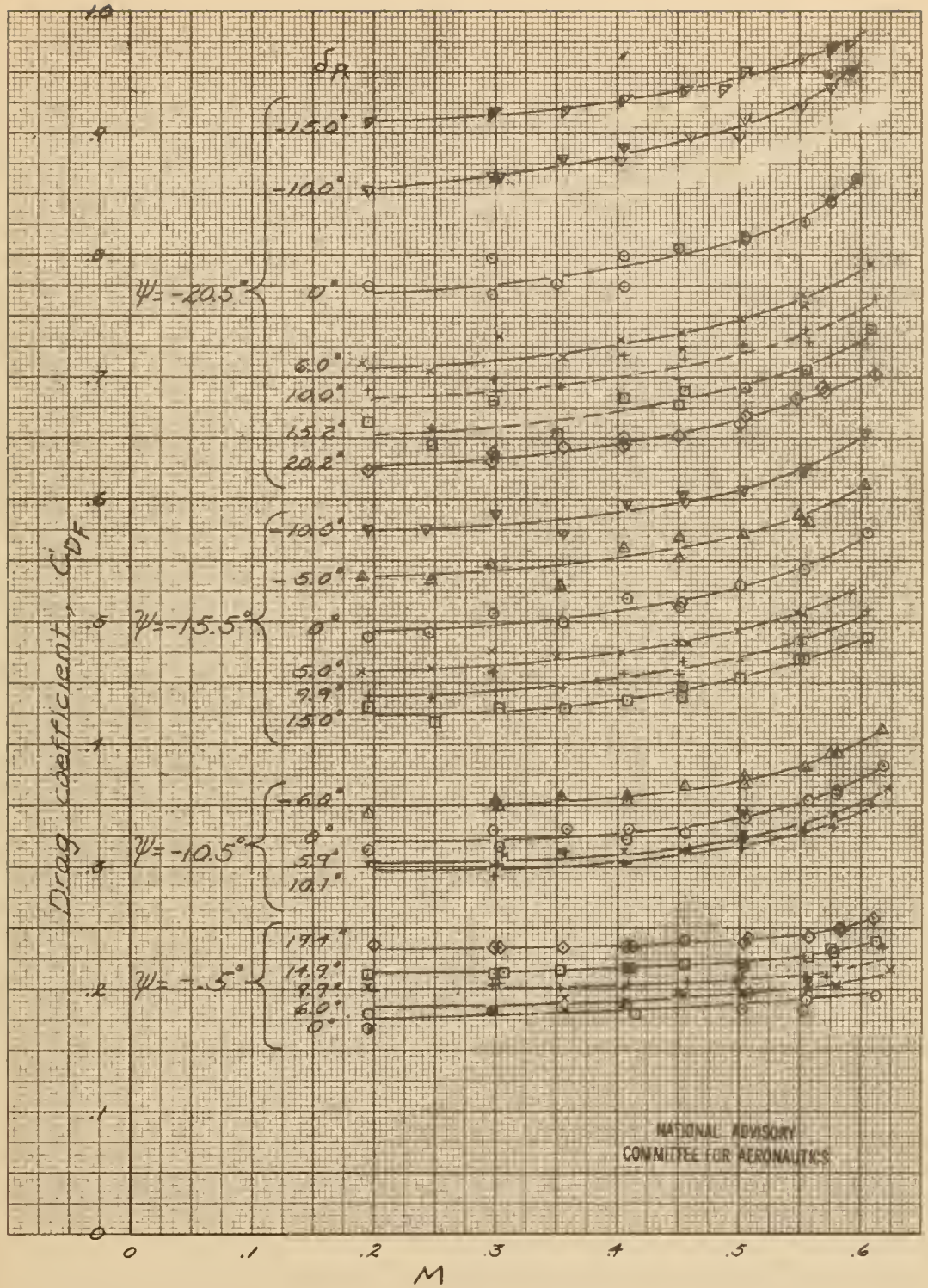

Figure 17.- Variation of drag coefficient with Mach number for several angles of sideslip and rudder angles.

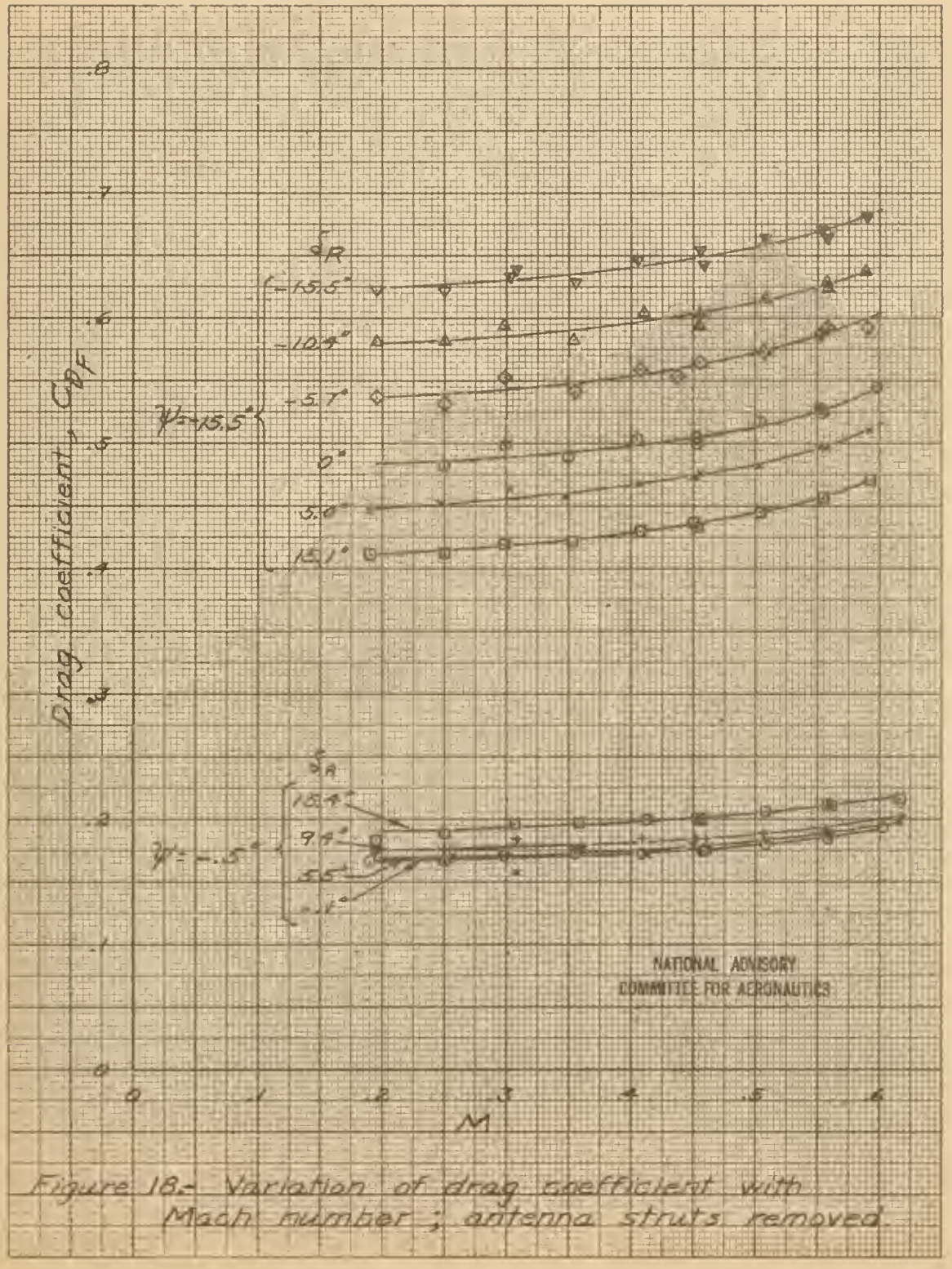

Figure 18.- Variation of drag coefficient with Mach number; antenna struts removed.

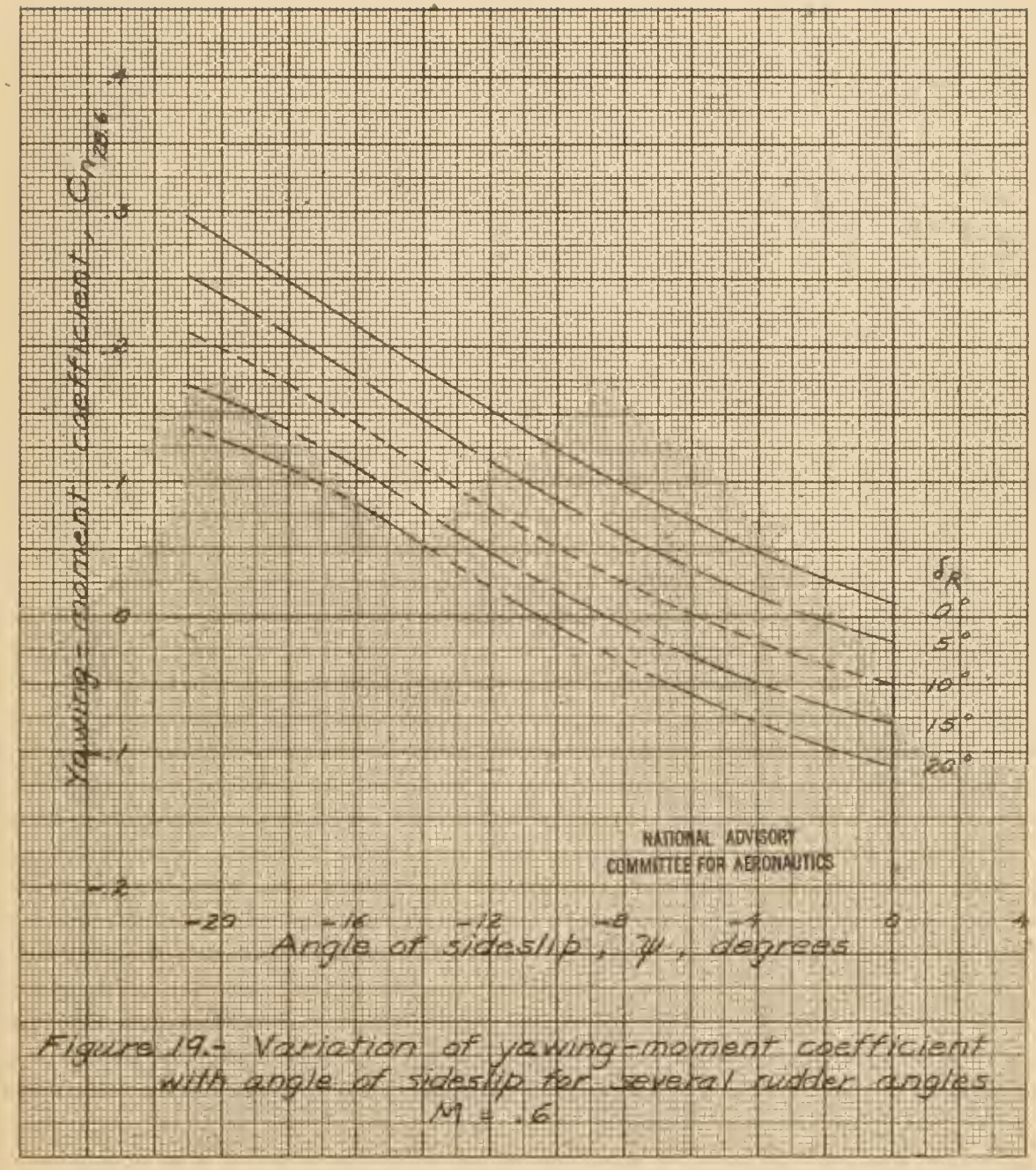

Figure 19.- Variation of yawing-moment coefficient with angle of sideslip for several rudder angles. $M_1 = .6$

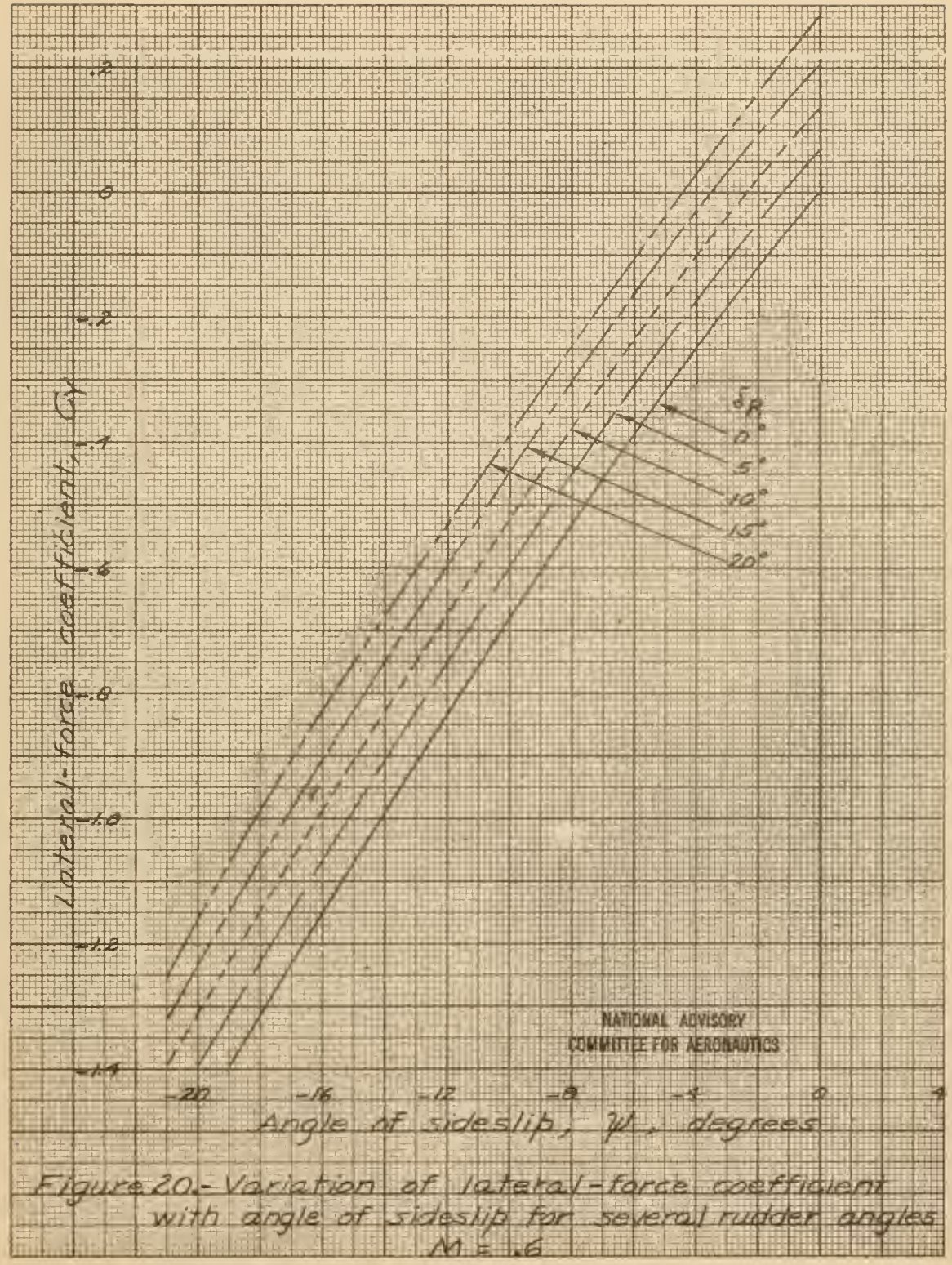

Figure 20.- Variation of lateral-force coefficient with angle of sideslip for several rudder angles M = .6

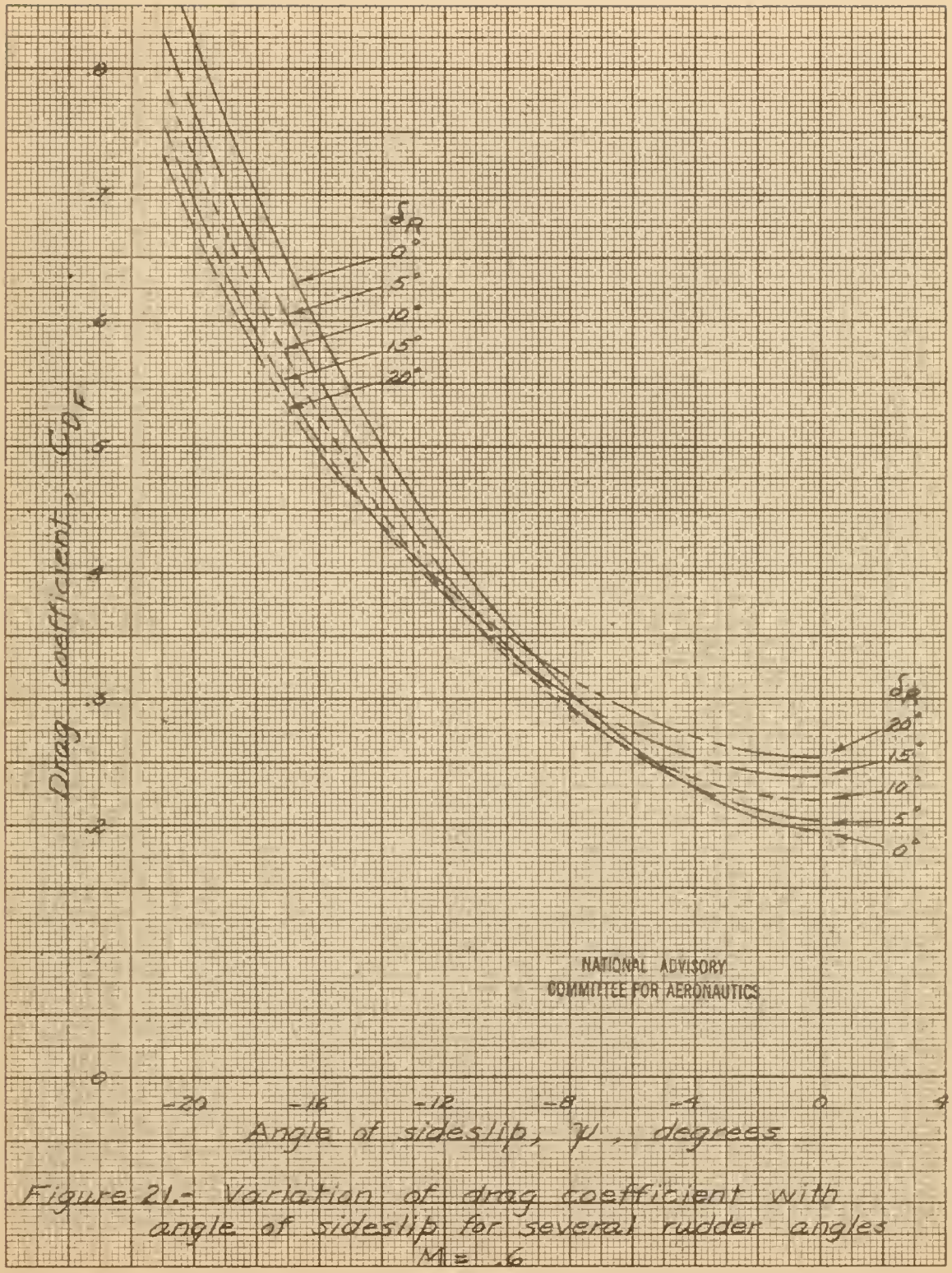

Figure 21.- Variation of drag coefficient with angle of sideslip for several rudder angles M = .6

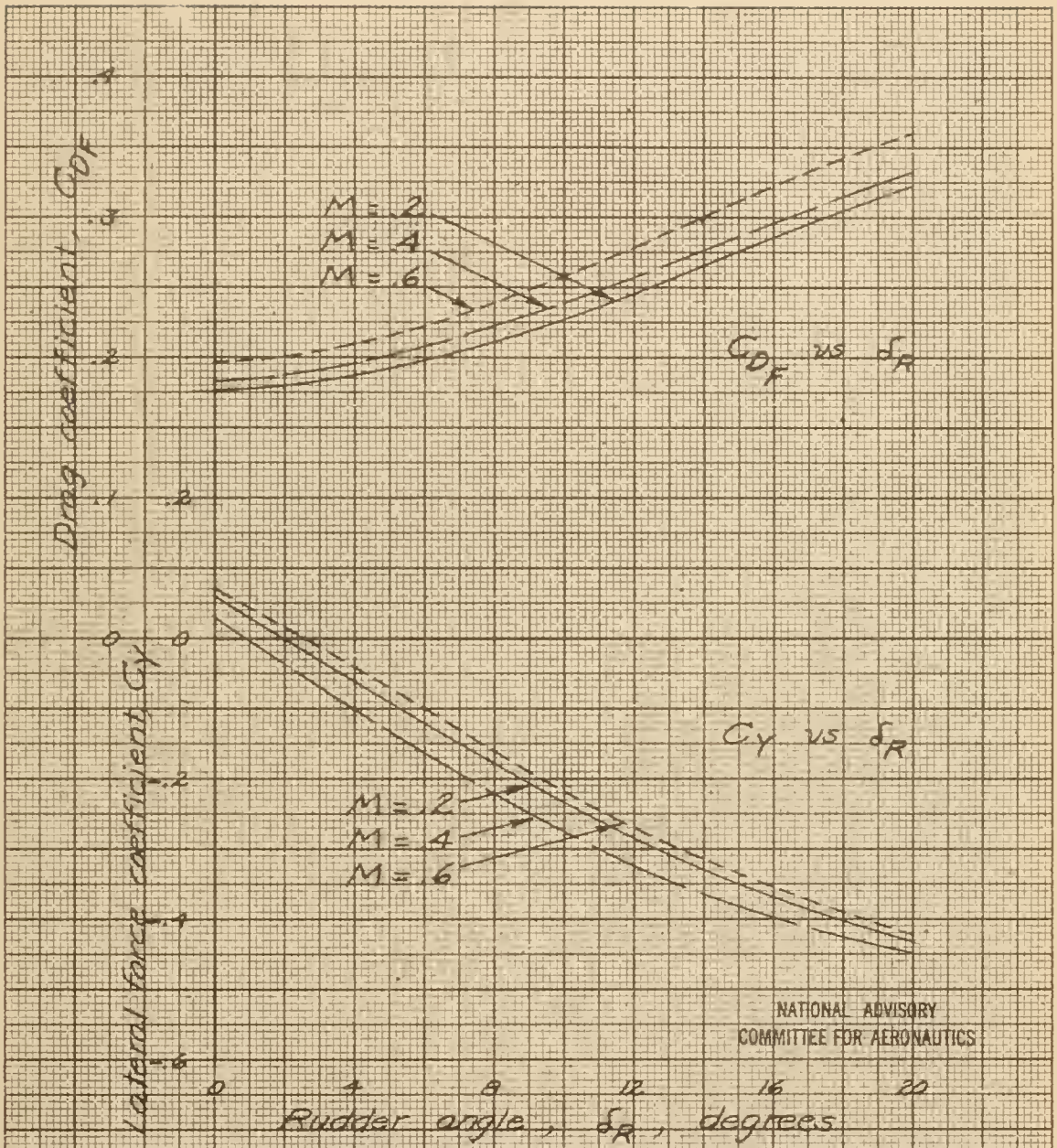

Figure 22.- Drag and lateral-force coefficients at trim versus the rudder angle for several Mach numbers.

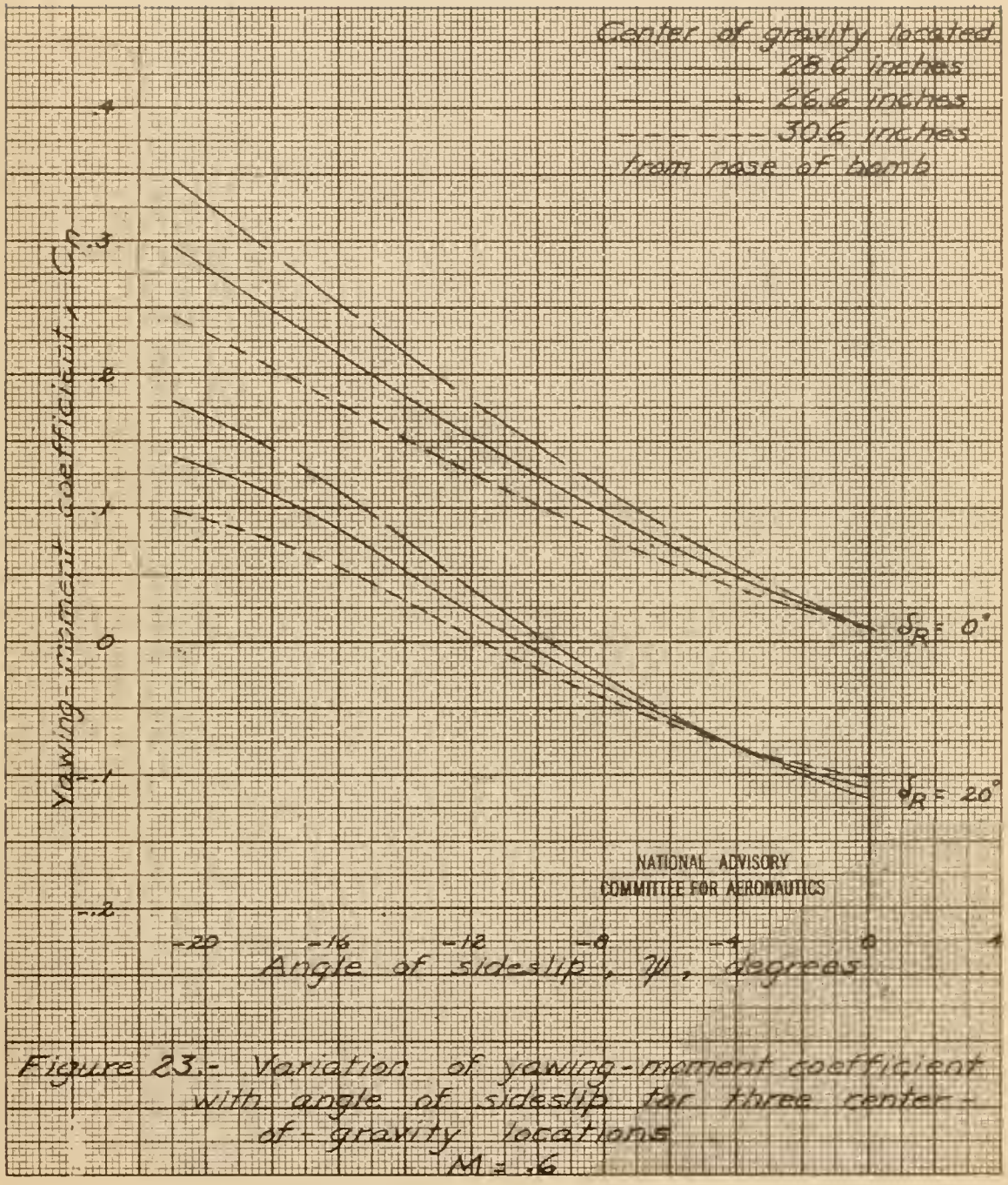

Figure 23.- Variation of yawing-moment coefficient with angle of sideslip for three center-of-gravity locations. $M = .6$

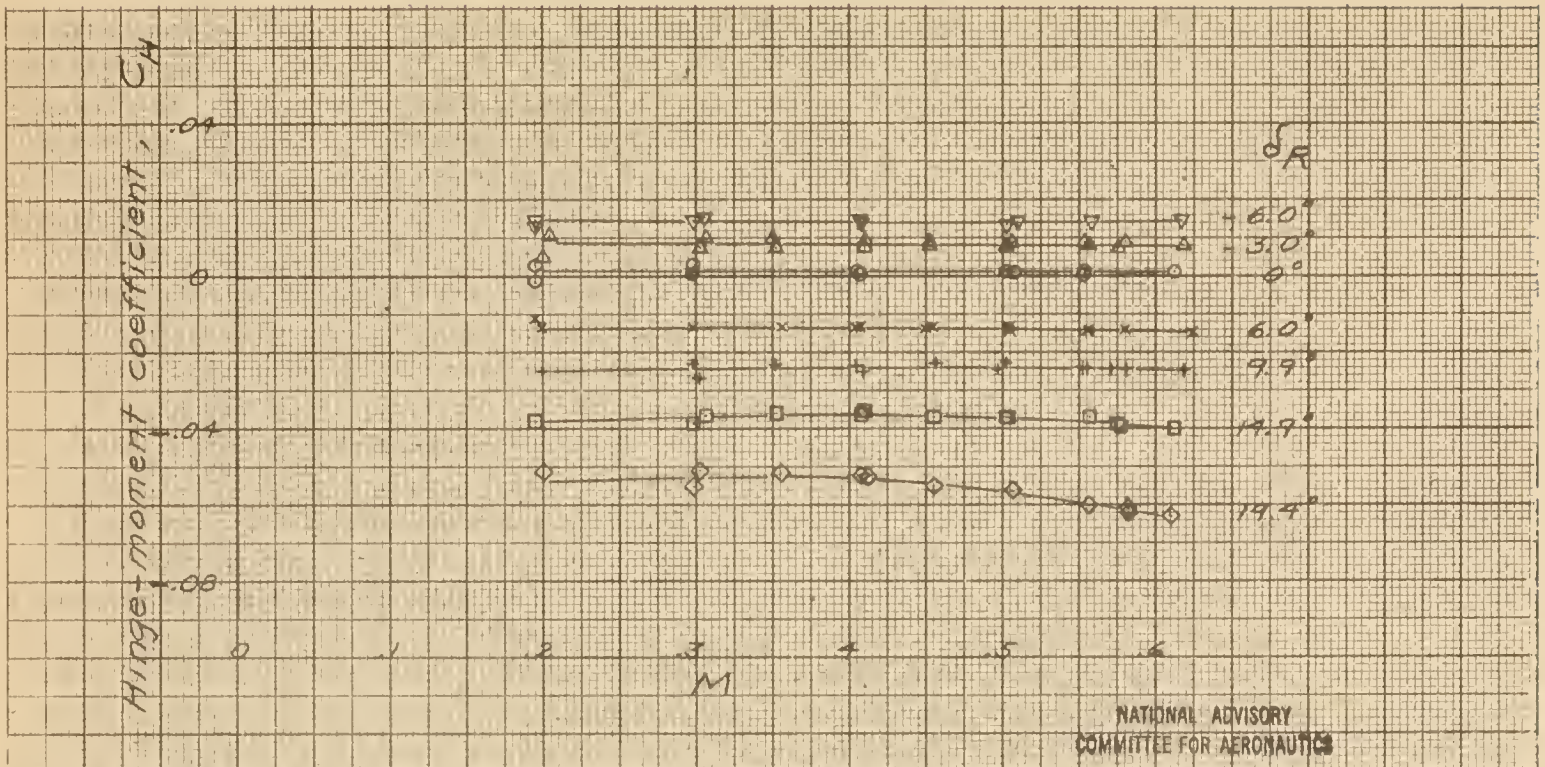

Figure 24.- Variation of rudder hinge-moment coefficient with Mach number for several rudder angles $\psi = -.5°$.

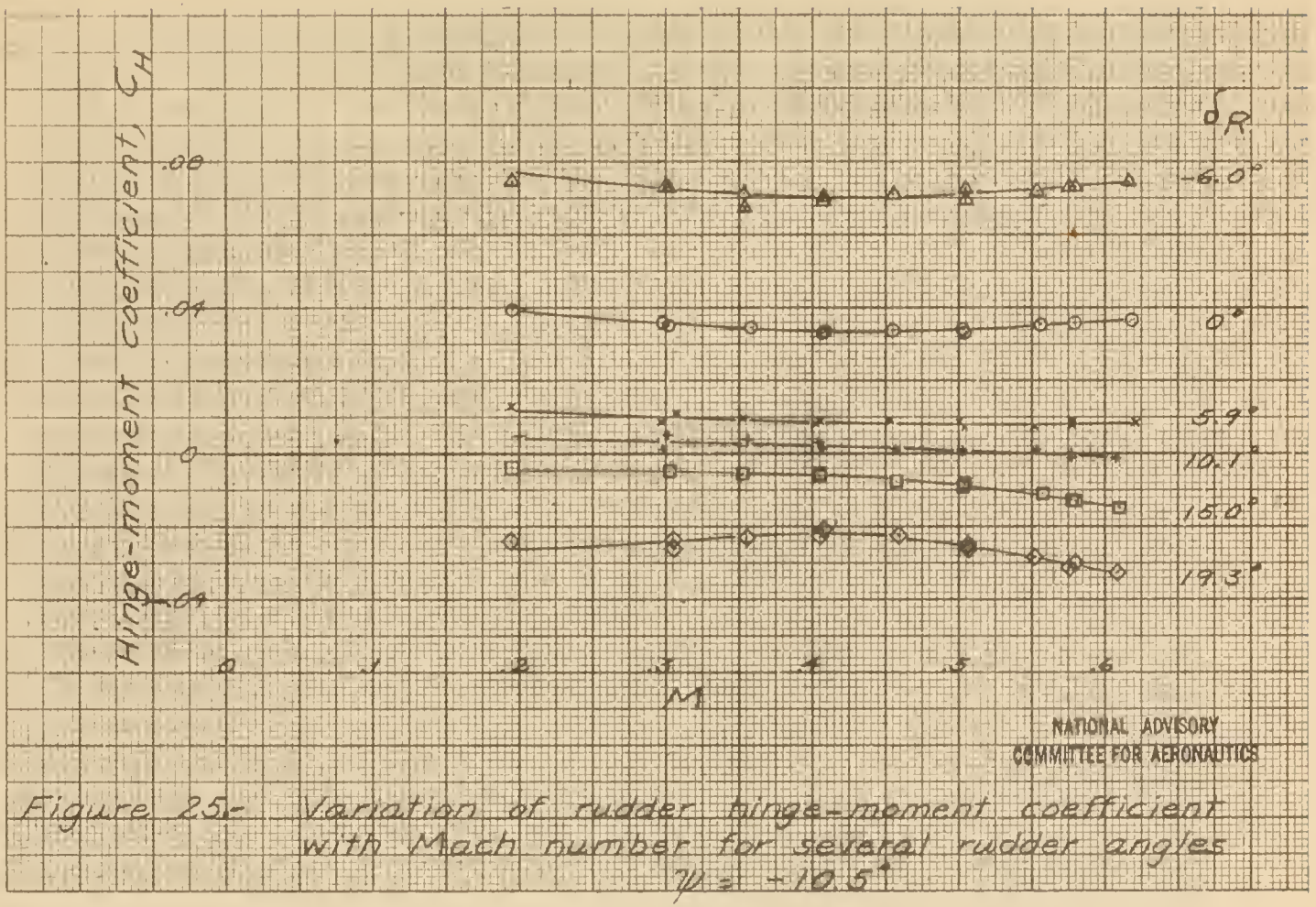

Figure 25.- Variation of rudder hinge-moment coefficient with Mach number for several rudder angles $\psi = -10.5°$

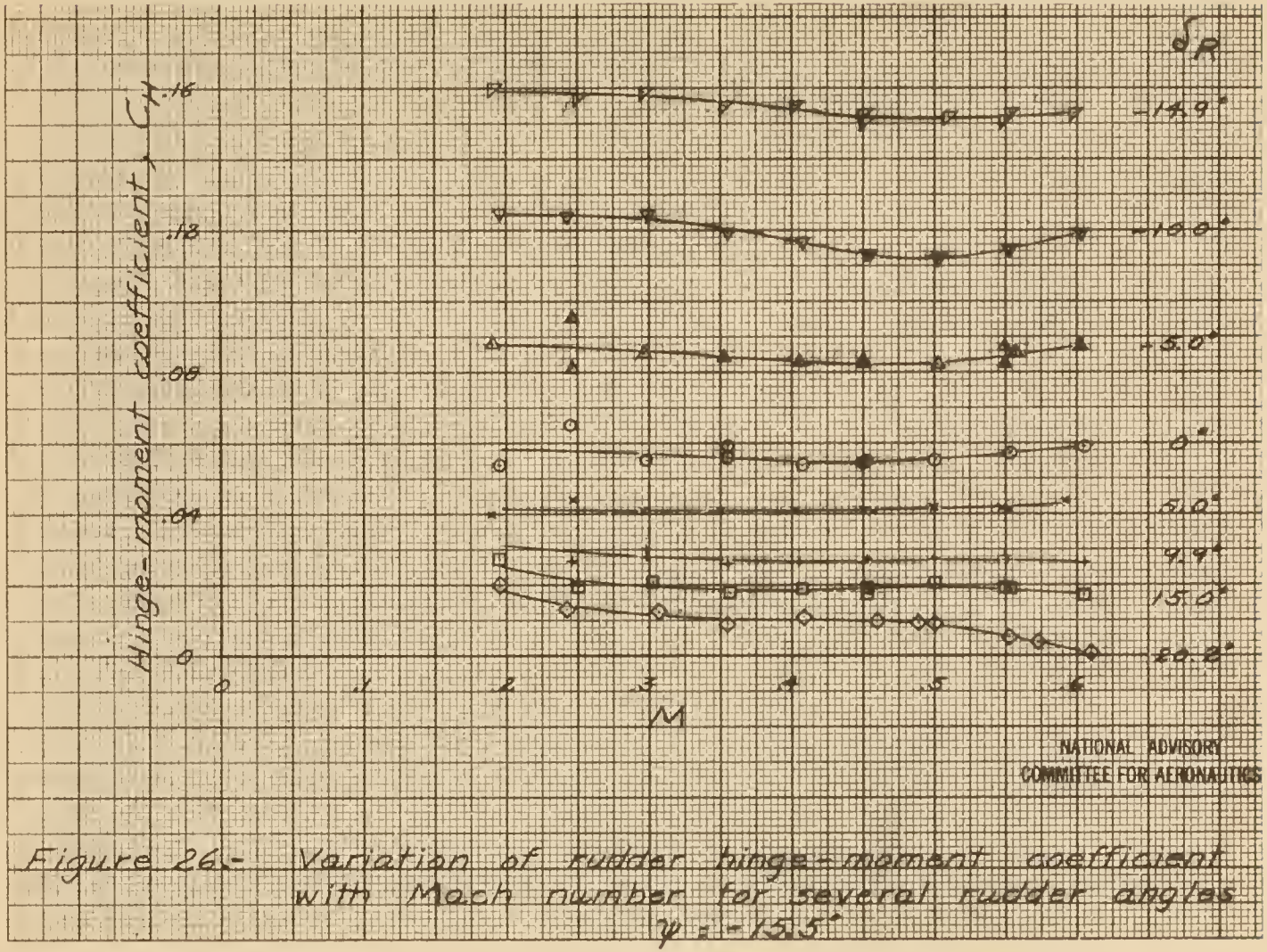

Figure 26.- Variation of rudder hinge-moment coefficient with Mach number for several rudder angles $\psi = -15.5°$

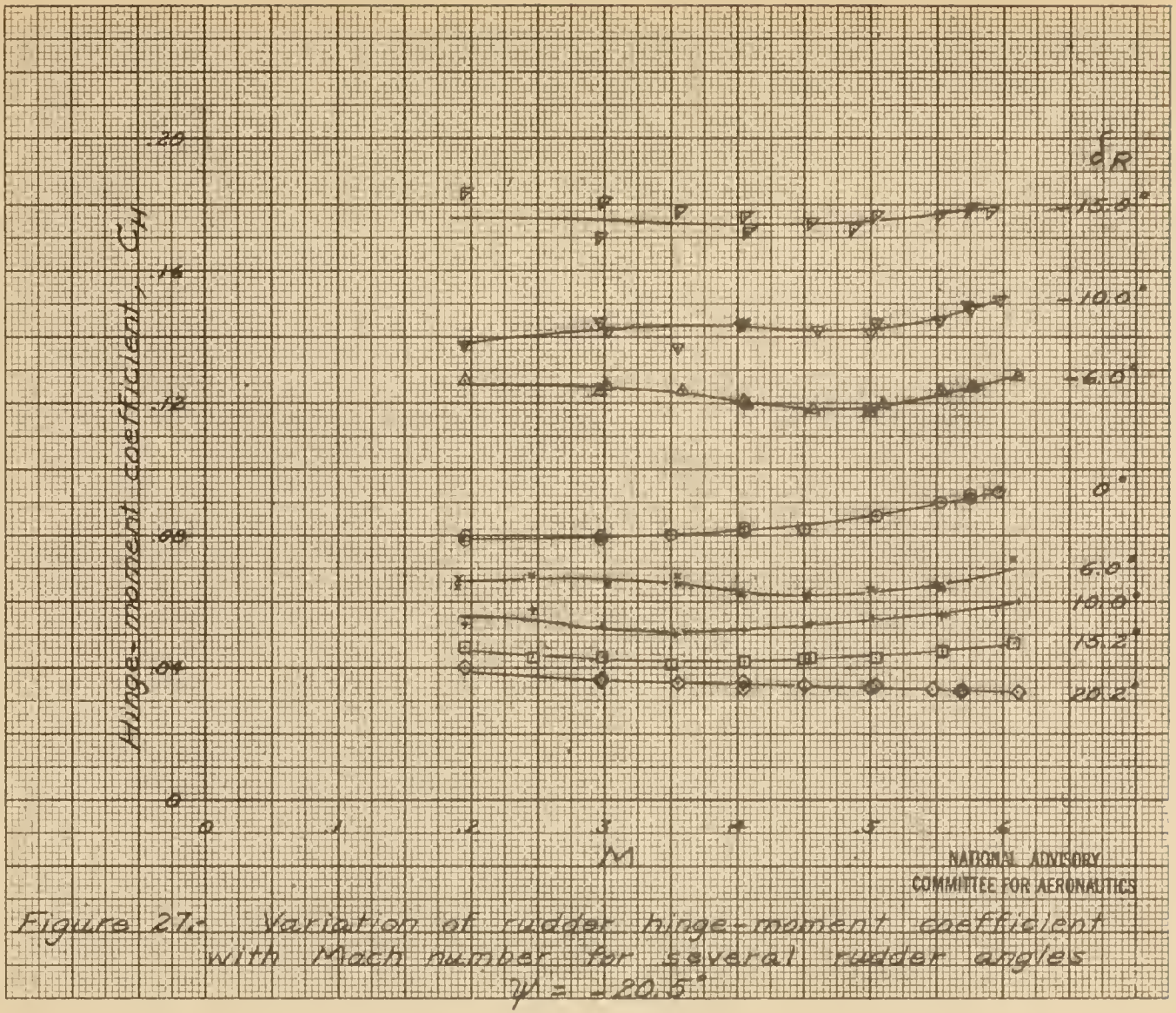

Figure 27.- Variation of rudder hinge-moment coefficient with Mach number for several rudder angles $\psi = -20.5°$

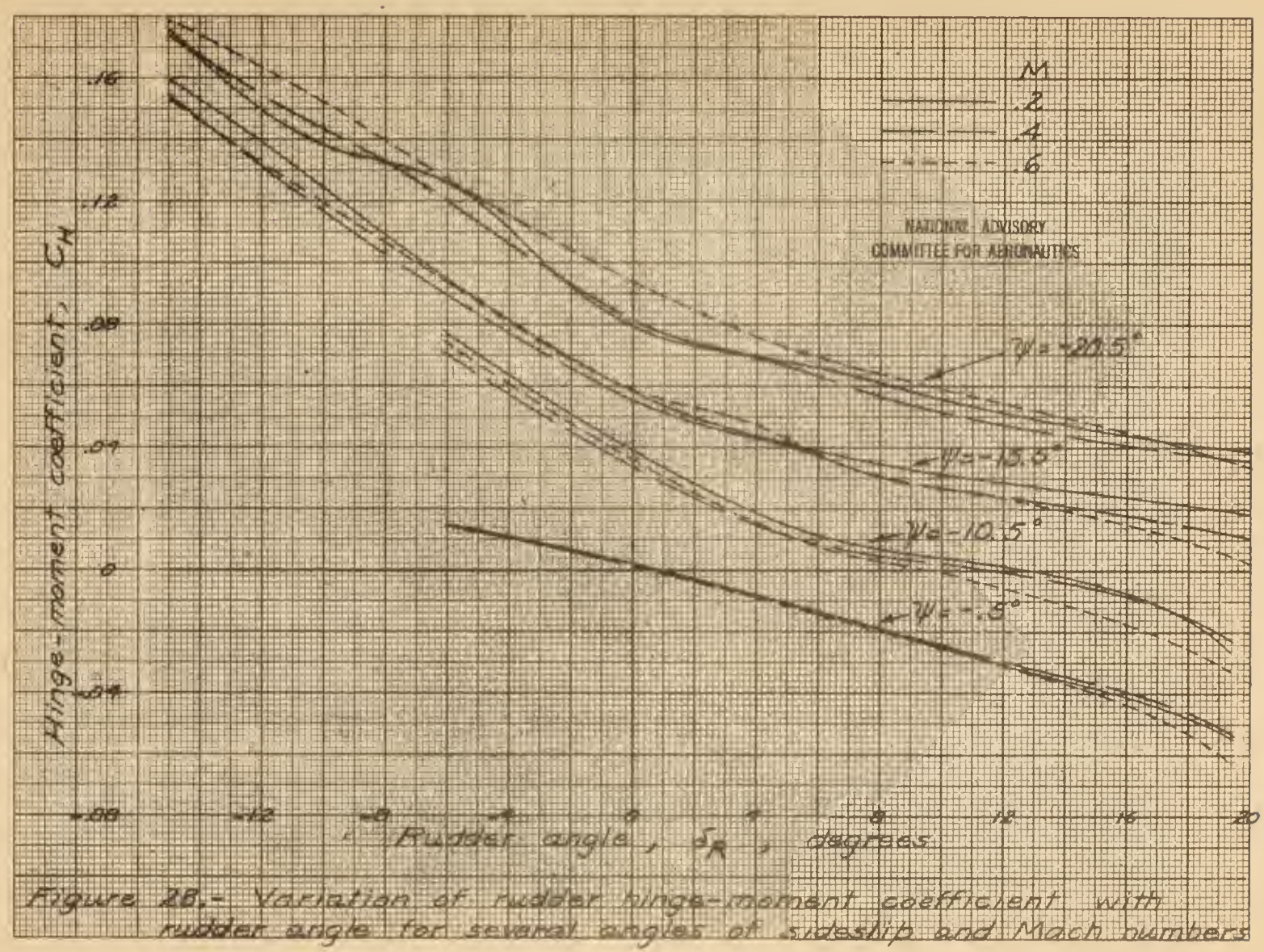

Figure 28.- Variation of rudder hinge-moment coefficient with rudder angle for several angles of sideslip and Mach numbers

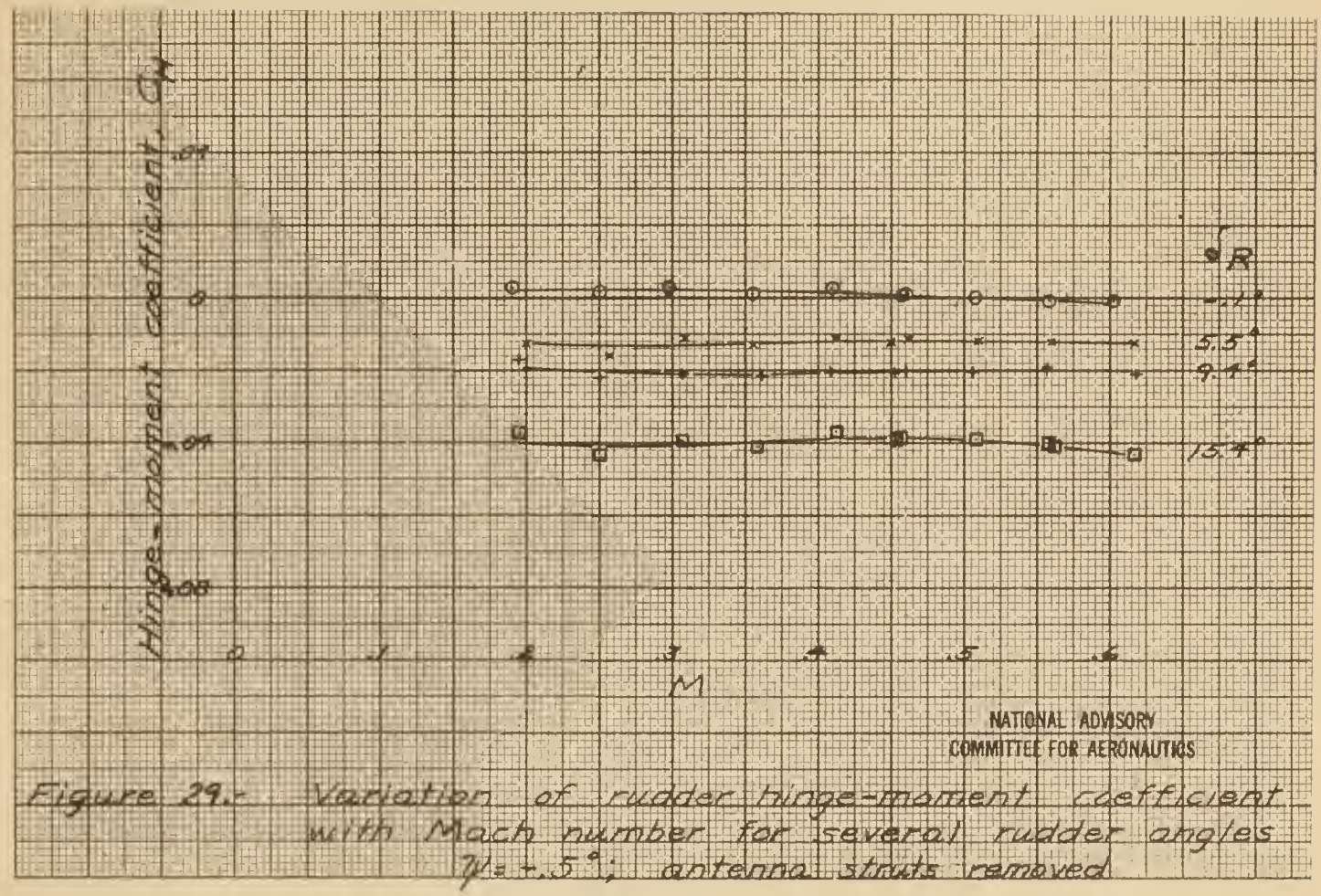

Figure 29.- Variation of rudder hinge-moment coefficient with Mach number for several rudder angles $\gamma_t = +.5°$; antenna struts removed

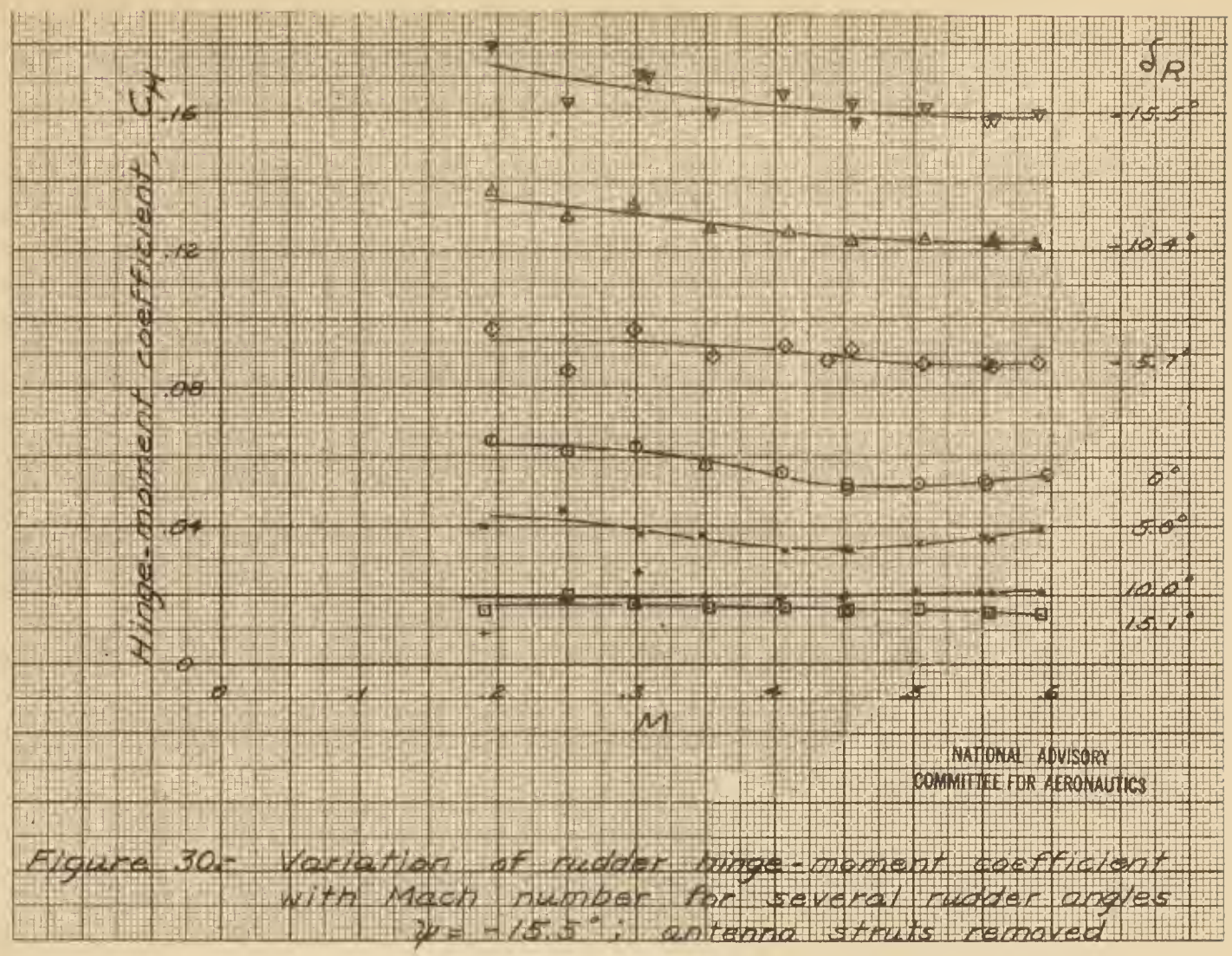

Figure 30.- Variation of rudder hinge-moment coefficient with Mach number for several rudder angles $\psi = -15.5°$; antenna struts removed

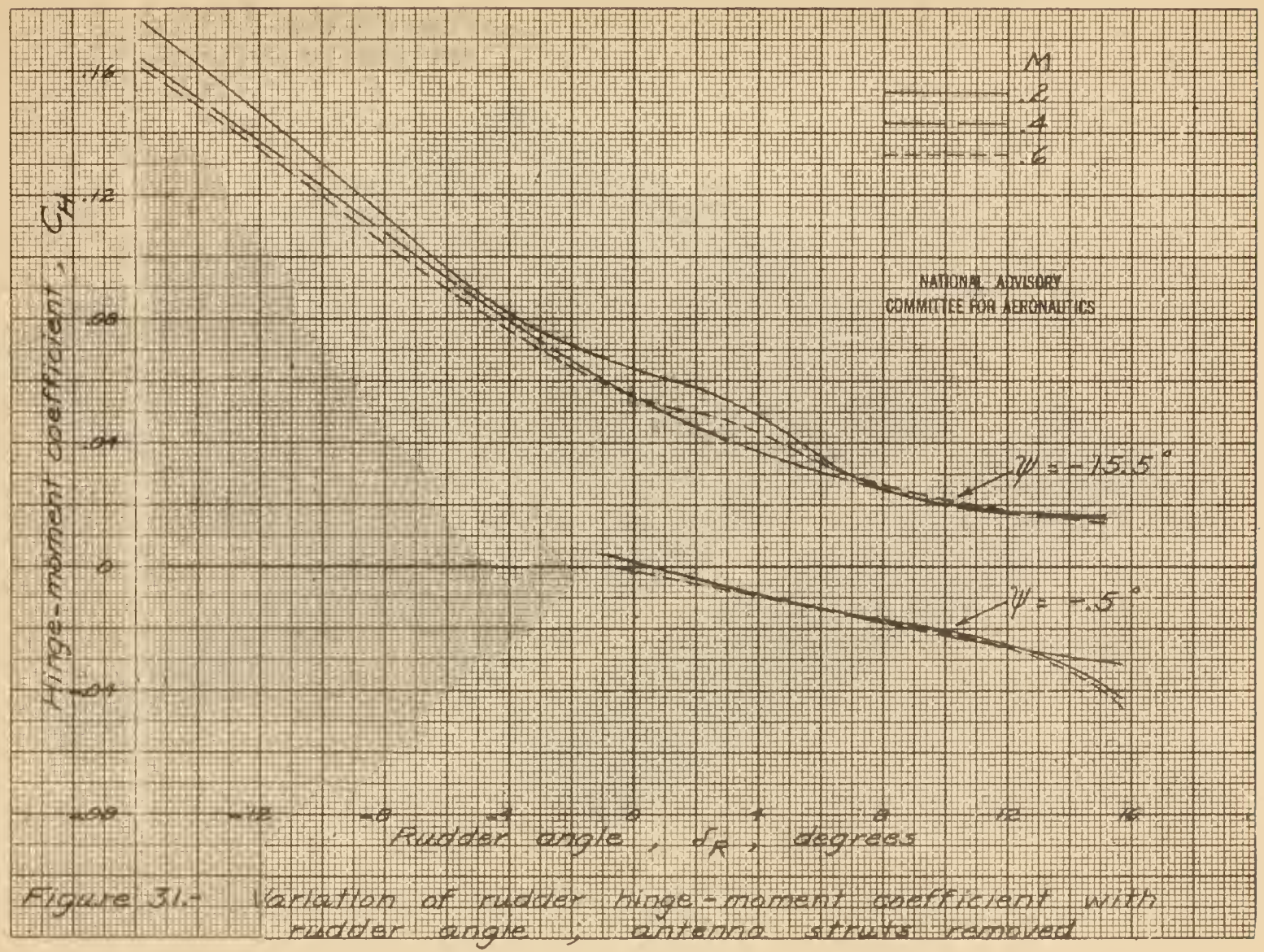

Figure 31.- Variation of rudder hinge-moment coefficient with rudder angle; antenna struts removed

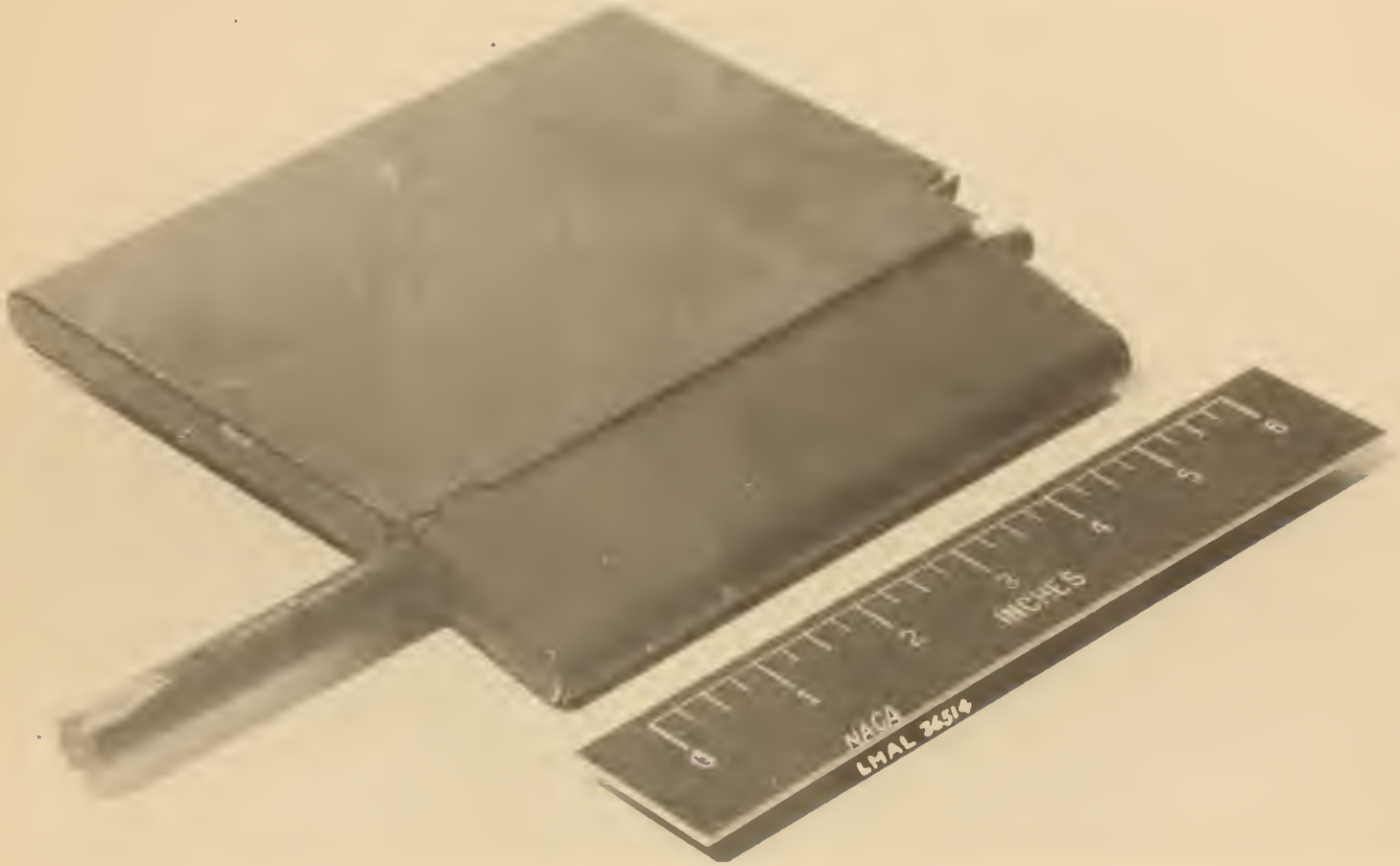

Figure 32.- Rudder failure.